



12-1996

Extensions of Green's Function Discretization for Modeling Acoustics in Inhomogeneous Media

Jonathan C. French
University of Tennessee

Follow this and additional works at: https://trace.tennessee.edu/utk_graddiss

Recommended Citation

French, Jonathan C., "Extensions of Green's Function Discretization for Modeling Acoustics in Inhomogeneous Media. " PhD diss., University of Tennessee, 1996.
https://trace.tennessee.edu/utk_graddiss/6114

This Dissertation is brought to you for free and open access by the Graduate School at TRACE: Tennessee Research and Creative Exchange. It has been accepted for inclusion in Doctoral Dissertations by an authorized administrator of TRACE: Tennessee Research and Creative Exchange. For more information, please contact trace@utk.edu.

To the Graduate Council:

I am submitting herewith a dissertation written by Jonathan C. French entitled "Extensions of Green's Function Discretization for Modeling Acoustics in Inhomogeneous Media." I have examined the final electronic copy of this dissertation for form and content and recommend that it be accepted in partial fulfillment of the requirements for the degree of Doctor of Philosophy, with a major in Engineering Science.

John E. Caruthers, Major Professor

We have read this dissertation and recommend its acceptance:

Accepted for the Council:

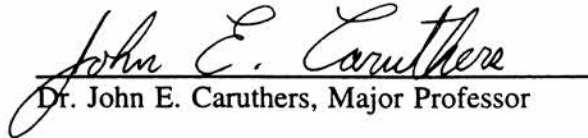
Carolyn R. Hodges

Vice Provost and Dean of the Graduate School

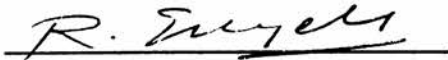
(Original signatures are on file with official student records.)

To the Graduate Council:

I am submitting herewith a dissertation written by Jonathan Charles French entitled "Extensions of Green's Function Discretization for Modeling Acoustics in Inhomogeneous Media." I have examined the final copy of this dissertation for form and content and recommend that it be accepted in partial fulfillment of the requirements for the degree of Doctor of Philosophy, with a major in Engineering Science.


Dr. John E. Caruthers, Major Professor

We have read this dissertation
and recommend its acceptance:







Accepted for the Council:


Associate Vice Chancellor and
Dean of The Graduate School

Extensions of Green's Function Discretization for
Modeling Acoustics in Inhomogeneous Media

A Dissertation

Presented for the

Doctor of Philosophy

Degree

The University of Tennessee, Knoxville

Jonathan C. French

December 1996

Copyright © Jonathan Charles French, 1997

All rights reserved

DEDICATION

This dissertation is dedicated to my wife,

Suzanne,

whom I love with all my heart,

and who has made my life complete.

ACKNOWLEDGMENTS

To paraphrase Sir Isaac Newton, I owe significant thanks to those whose shoulders supported me as I conducted the research embodied in this dissertation. Above all, I am indebted to Dr. John Caruthers, whose insight and vision led to both practical and theoretical avenues of research. In addition, I would like to thank Dr. G.K. Raviprakash, a UTSI research engineer for his patient endurance of lengthy theoretical discussions, and my dissertation committee, Dr. John Caruthers, Dr. Remi Engels, Dr. K.C. Reddy and Dr. Robert Roach, for their support and guidance. Finally, I would like to thank my parents, Charles and Barbara French, who have encouraged me in all of my endeavors.

ABSTRACT

This research examines two new methods to numerically model linear field equations with spatially varying coefficients, with a particular focus on the acoustic velocity potential equation. The methods are based on a new field discretization technique, Green's function discretization (GFD), which was primarily developed to model the Helmholtz equation for frequency domain acoustics problems in homogeneous media. GFD can be used to model acoustics in inhomogeneous media by assuming constant media properties across each computational stencil. The methods presented herein correct GFD for variations in the media across each stencil in two distinct ways: via a Fredholm volume integral, and by a particular solution to a perturbation expansion. To evaluate these methods, boundary value problem test cases have been numerically evaluated to determine gains in accuracy in one and two dimensions. The results demonstrate that the ability of GFD to model the effects of an inhomogeneous medium on acoustics can be significantly increased using corrections factors computed from these new methods.

TABLE OF CONTENTS

CHAPTER 1. INTRODUCTION	1
1.1. Background	3
1.2. Current Methodology Classification	6
CHAPTER 2. DERIVATION AND METHODOLOGY	7
2.1. Local Fredholm Integral Formulation	8
2.2. Second Order Perturbation Expansion Method	19
CHAPTER 3. IMPLEMENTATION RESULTS	29
3.1. Description of Tests Performed	29
3.2. Explanation of Error Plots	30
3.3. 1-D Linearly Varying Reduced Frequency Cases	31
3.4. 2-D Bessel Function "Bump" Reduced Frequency Cases	41
CHAPTER 4. CONCLUSIONS	50
CHAPTER 5. FURTHER WORK	52
LIST OF REFERENCES	53
APPENDICES	56
APPENDIX A: DERIVATION OF THE ACOUSTIC VELOCITY POTENTIAL EQUATION (AVPE) WITH ISENTROPIC AND IRROTATIONAL STEADY FLOW	57
APPENDIX B: DERIVATION OF THE NTH ORDER ACOUSTIC VELOCITY POTENTIAL PERTURBATION EQUATION	70
APPENDIX C: DERIVATION OF THE PARTICULAR SOLUTION TO 2-D QUADRATIC LAGRANGIAN INTERPOLATION FUNCTIONS	72
VITA	78

LIST OF FIGURES

FIGURE	PAGE
1. Volumes and surfaces in the Fredholm integral formulation	9
2. Discretized single layer potential on surface S_0	15
3. 1-D Computational mesh and frequency distribution	32
4. 1-D Method comparison, $H = 0.01$	34-35
5. 1-D Method comparison, $H = 0.1$	36-37
6. 1-D Method comparison, $H = 1.0$	38-39
7. 1-D Method comparison for varying values of H	40-41
8. 2-D Computational mesh, and inhomogeneous media region	43
9. 2-D Method comparison, $H = 0.01$	44-45
10. 2-D Method comparison, $H = 0.1$	46-47
11. 2-D Method comparison, $H = 1.0$	48-49

NOMENCLATURE

\vec{a}	Denotes a vector
a_i	Denotes i^{th} component of vector \vec{a} (tensor notation)
a_{ij}	Denotes i^{th} row and j^{th} column of matrix A
a_{ij}^{\dagger}	Denotes i^{th} row and j^{th} column of pseudo-inverse matrix A
B_i	Spatially varying tensor coefficient of the acoustic velocity potential equation's gradient term
C	Spatially varying coefficient in the acoustic velocity potential equation
c	Speed of sound
c_k	Plane wave coefficient
G	Infinite space Green's function
H	Sum of a Green's function and inhomogeneous media correction factors
H	Perturbation size parameter
i	$\sqrt{-1}$
J_0	Bessel function of first kind, order 0
J_1	Bessel function of first kind, order 1
k	Reduced frequency ($\omega L/c$)
L	Length parameter

M	Mach number
M_i	Spatially varying Mach vector ([velocity vector] / [speed of sound]
\vec{n}	Unit vector perpendicular from a surface (normal)
q_{ki}	Plane wave frequency term that accounts for locally constant steady flow coefficient terms
P	Polynomial that models variation of steady flow variables across computational stencil
\vec{p}	Coefficients of polynomial P
p	Pressure
R	Polynomial used to form a particular solution to the acoustic velocity potential equation with a P polynomial forcing function
\vec{r}	Coefficients of polynomial R
r	Amplitude of the acoustic potential
s	Entropy
t	Time variable
v_{kj}	Unit vector (k unit vectors with j components)
x,y,z	Spatial coordinates
\vec{v}	Velocity vector
θ	Phase of the acoustic potential
ϵ	Perturbation parameter
ϕ	Acoustic velocity potential

- ρ Density
- σ Single layer potential source strength
- ω Angular frequency (radians/time)
- $\vec{\omega}$ Vorticity vector

LIST OF ABBREVIATIONS

AVPE Acoustic Velocity Potential Equation

BEM Boundary Element Method

GFD Green's Function Discretization

PDE Partial Differential Equation

SVD Singular Value Decomposition

CHAPTER 1

INTRODUCTION

Noise pollution regulations and competition between manufacturers are driving engineers to develop products with noise minimization as part of the design iteration loop. From automobiles to aircraft engines, manufacturers are attempting to gain a competitive edge by making their products as quiet as possible, or at least quiet enough to meet government ordinances. Following a trend set by structural analysis, computational acoustics codes are being applied in the design loop to reduce the number of experimental design analyses. This dissertation presents a new numerical method, based on fundamental acoustics principles, which has the potential to dramatically accelerate the design iteration process.

Sound propagation is mathematically modeled using the wave equation:

$$\frac{1}{c^2} \frac{\partial^2 \bar{\phi}}{\partial t^2} = \nabla^2 \bar{\phi} \quad (1)$$

$\bar{\phi}$ is the acoustic potential and c is the speed of sound. If a noise is dominated by particular frequencies, a practical mathematical model can be obtained by Fourier-decomposition. The wave equation is reduced to the Helmholtz equation by assuming harmonic time (t) variation ($\bar{\phi} = \phi e^{i\omega t}$):

$$\nabla^2 \phi + \frac{\omega^2}{c^2} \phi = 0 \quad (2)$$

The noise's spatial attributes are then determined by solving the Helmholtz equation over the region of noise emission for each discrete frequency (ω) of interest. Analytical solutions are only available for simple geometries, so a numerical solution is generally required. To reduce potentially long computation times, it is necessary to choose the "best" numerical technique to solve the problem. For this study, the "best" method must be both accurate and fast: reduce one criterion and the method can be quickly rendered useless by the complexity of the problem.

The boundary element method (BEM) is a potential option for problems without variations in the acoustic media. However, when the acoustic medium changes, as when a steady flow field is present or thermodynamic properties vary spatially, a field discretization is required. There are two inherent problems with field discretizations: second order methods require ten computational nodes per wavelength per dimension to accurately resolve the acoustics (higher order methods claim 6-8 nodes / wave / dimension), and they require that the computational domain be extended into the far-field to prevent acoustic energy from being reflected back into the computational domain. In multiple dimensions, these requirements result in lengthy computation times, dominated by the solution of large banded matrices. Accordingly, frequency domain acoustics computations have been generally limited to only two dimensions.

To alleviate these computational requirements, a new numerical technique, the Green's function discretization (GFD) method, has been developed to provide a radiation

boundary condition that allows acoustic energy to exit the domain in the near field, drastically reducing the overall size of the computational domain [1]. When GFD is applied to the interior discretizing process, the resulting solution is quite accurate using fewer than three computational nodes per wavelength per dimension [2]. Since the computational effort required to solve an implicit system of equations with n nodes per dimension is $O(n^4)$ in two dimensions, and $O(n^7)$ in three dimensions, significantly reducing the number of nodes per dimension results in an exponential time savings [4]. While GFD is not a tool that can accelerate the solution of every computational problem, it can, when used appropriately, make previously intractable problems manageable. This dissertation will focus on applications that cannot be solved using boundary element methods: multi-dimensional inhomogeneous acoustic medium problems involving the variable coefficient Helmholtz equation. The medium will be assumed to have continuous properties (i.e. continuous variable coefficients).

1.1 Background

The underlying reason for the success of the Green's function discretization can be summed up in the following quote by Pierce [3]:

"... there is some historical precedent to believe that any scheme that incorporates more of the basic physical understanding of how waves

propagate should have some intrinsic advantages over one based on brute force."

As a wave propagates, its amplitude and phase vary continuously as it travels through space, as do most of the wave's spatial derivatives. Numerical schemes which assume some form of Taylor series "truncation error" of higher order terms, or approximate the wave's shape using polynomial functions, require a dense mesh to model the wave's constantly changing shape. GFD has been derived strictly from boundary integral equations, which take into account the full nature of wave propagation. The GFD process utilizes locally exact solutions with a formal truncation error of zero, and the result has been the development a new dispersionless numerical method.

GFD was first implemented as a near-field radiation boundary condition by Raviprakash [1] to model noise propagation from a turbofan engine inlet. The interior field equations were approximated by a finite volume discretization. By allowing the noise to radiate from the near-field, the size of the computational domain was dramatically reduced without compromising the solution or introducing any non-physical computational tricks.

The multi-dimensional application of GFD to the interior of the computational domain was explored by French [2], propelled by the fact that the 1-D application of GFD is exact. The results demonstrated that the method was uncommonly accurate with three computational nodes per wave in 2-D. At this time, the effective limit of the method was

observed by Engels¹ to be the resonant frequency of the local stencil. A complete documentation of the GFD method for the Helmholtz equation, which includes an extension of the method for post-solution interpolation, is given by Caruthers, French and Raviprakash [4], and includes a comparison of the computational work required by the BEM and field discretizations.

A Neumann boundary condition was formulated using GFD, and was used to model a 2-D piston in conjunction with a pseudo-3D ring source method by Caruthers and Raviprakash [5]. This work was followed by a paper by Caruthers, French and Raviprakash that elucidated the details for the application of Neumann boundary conditions, demonstrated GFD's ability to handle skewed and irregular meshes, and presented a new technique for embedding boundaries in Cartesian meshes [6].

The first step toward approximating the effects of a spatially varying steady flow on the acoustics was to consider the acoustic equation's steady flow coefficients to be constant over each stencil [Caruthers, Engels and Raviprakash, 7], yielding a method which gave only first order consideration to steady flow variations. This was accomplished by using plane waves instead of Green's functions in multiple dimensions. The purpose of this dissertation is to extend the work presented in [7] by identifying and examining methods that approximate the second order effects of the steady flow variations on the acoustics.

¹UTSI Engineering Science professor

1.2. Current Methodology Classification

Different approximation techniques for dealing with variable coefficient equations of the type considered are classified by the non-dimensional reduced frequency parameter, $k = \omega L/c$. ω is the circular frequency in radians/sec, L is the problem's length scale (the grid spacing, in this case), and c is the speed of sound. Low frequency ($k^2 \ll 1$) approximations assume that the Helmholtz equation can be approximated by the Laplace equation, by interpreting k^2 as a perturbation quantity [8, p. 1085]. Conversely, high frequency ($k^2 \gg 1$) approximations, such as the WKBJ approximation, assume that $1/k^2$ is the perturbation quantity [8, p. 1092]. The case to be dealt with in this dissertation assumes that $k^2 \approx 1$. For this case, the frequency parameter cannot be assumed to be a perturbation, and a different approach must be taken. Commonly, the local constant coefficient solution is used as a starting point to compute higher order solutions, either iteratively (as in Rayleigh-Gans [8, p. 1073 and 9, p. 321]) or by successive terms of a formal perturbation expansion. The two numerical methods to be presented follow these approaches.

CHAPTER 2

DERIVATION AND METHODOLOGY

This discussion will be directed toward the field of aero-acoustics, although other similar applications are available. In aero-acoustics, a steady state flow field is initially computed over the region of interest. The acoustics can then be computed taking the steady flow into account. When the steady flow field is isentropic and irrotational, the acoustic velocity potential equation (AVPE) can be restated to include the flow field effects in terms of a Mach vector ($\vec{M} = \vec{v}/c$, \vec{v} is the steady flow velocity vector) and the reduced frequency (k):

$$[\delta_{ij} - M_i M_j] \phi_{,ij} - 2[M_j M_{i,j} + i M_j k] \phi_{,i} + [k^2 - i M_j k_{,j}] \phi = 0 \quad (3)$$

$$\delta_{ij} = \begin{cases} 1, & i=j \\ 0, & i \neq j \end{cases}$$

Note that Cartesian tensor notation is invoked, and that the variable coefficients are functions of the steady flow field. The derivation of this equation is presented in Appendix A. To generalize this equation, it will be cast in the following form to separate the constant and non-constant coefficients:

$$[\delta_{ij} - M_i M_j] \phi_{,ij} + B_i \phi_{,i} + [k^2 + C] \phi = 0 \quad (4)$$

The Green's function discretization was derived from boundary integral methods, and as such is highly accurate for problems with uniform flow. When a spatially varying

steady flow field or temperature variations are introduced, the AVPE's coefficients change to reflect the effects of the medium variations on the sound waves. GFD's highly accurate discretization for homogenous media will be used as a starting point to generate discretizations for inhomogeneous media problems.

An important factor in this transition from homogeneous to inhomogeneous media is the observation that GFD can be used to interpolate only within the local computational stencil, as the interpolation becomes inaccurate outside the stencil. This implies that only the variations in the acoustic medium within the local stencil itself need to be taken into account. Variations in the acoustic medium outside the bounds of the local stencil may be ignored for each individual discretization. This observation will be used to derive two different approximation methods which both yield correction terms for the Green's function: a local Fredholm integral, and a local particular solution.

2.1. Local Fredholm Integral Formulation

The Fredholm integral modification to a Green's function is derived from a rigorous adherence to the original boundary integral formulation of GFD, and results in a method referred to as a Rayleigh-Gans approximation [9, p. 321] (a.k.a. Born approximation [8, p. 1073]). In this formulation, the AVPE shall be expressed as:

$$\phi_{,i}(\bar{x}_d) + k^2\phi(\bar{x}_d) - M_i M_j \phi_{,ij}(\bar{x}_d) + B_i \phi_{,i}(\bar{x}_d) + C\phi(\bar{x}_d) = 0 \quad (5)$$

To simplify the problem for this formulation, $M_i M_j$, B_i and C will be assumed to be of perturbation size, although in general $M_i M_j$ and B_i are not. The constant coefficient's free field Green's function is determined from the equation:

$$\nabla_d^2 G(\bar{x}_d; \bar{x}) + k^2 G(\bar{x}_d; \bar{x}) = -\delta(\bar{x}_d - \bar{x}) \quad (6)$$

This derivation follows the original derivation of the Green's function discretization. In figure 1, the square region (V_1) is a volume covering a computational stencil. It is enclosed in surface S_1 . Surface S_1 is enclosed by surface S_0 , and between surface S_0 and S_1 is a second volume region, V_2 . The volume outside surface S_0 is denoted as V_3 . Let $V_0 = V_1 \cup V_2$.

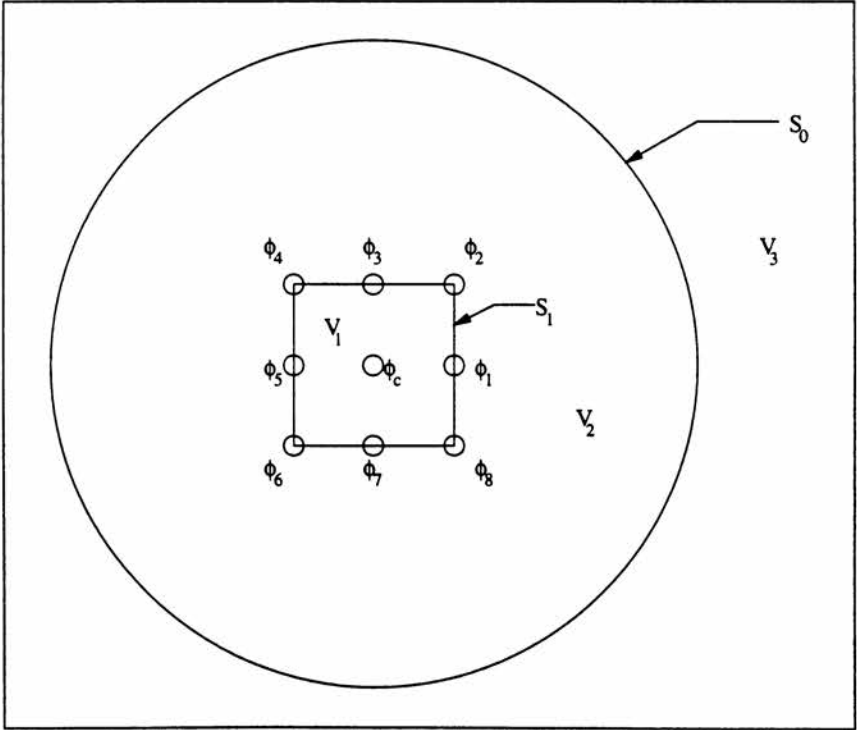


Figure 1. Volumes and surfaces in the Fredholm integral formulation

The acoustic potential inside V_1 (ϕ_c) can be interpolated within the square region (V_1) using GFD, from knowledge of incoming waves from the neighboring ϕ_j ($j=1-8$) nodes. Notably, ϕ_c can be interpolated only within V_1 ; extrapolation into the V_2 (and V_3) volumes using the same ϕ_j neighbors becomes quickly inaccurate. We will contain the effects of the local inhomogeneous media within V_1 in a Fredholm integral.

The formal derivation begins with Green's Identity:

$$\int(\nabla_d \cdot \vec{F})dV_d = \int(\vec{n}_d \cdot \vec{F})dS_d \quad (7)$$

The d subscript refers to the function dependence on a "dummy" variable that is used in the integration. This equation is true for each volume (V_0, V_1, V_2, V_3) and its bordering surfaces.

Let $\vec{F} = \phi_1 \nabla \phi_2 - \phi_2 \nabla \phi_1$; then

$$\nabla \cdot \vec{F} = \phi_1 \nabla^2 \phi_2 - \phi_2 \nabla^2 \phi_1 \quad (8)$$

Substituting equation 8 into equation 7:

$$\int[\phi_1 \nabla_d^2 \phi_2 - \phi_2 \nabla_d^2 \phi_1]dV_d = \int \vec{n}_d \cdot [\phi_1 \nabla_d \phi_2 - \phi_2 \nabla_d \phi_1]dS_d \quad (9)$$

Let $\phi_1 = \phi(\vec{x}_d)$, and $\phi_2 = G(\vec{x}_d; \vec{x})$. These two variables come from the AVPE and Green's function equation, given in equations 5 and 6, which can be rearranged as:

$$\nabla_d^2 \phi(\vec{x}_d) = -k^2 \phi(\vec{x}_d) + M_i M_j \phi_{,ij}(\vec{x}_d) - B_i \phi_{,i}(\vec{x}_d) - C \phi(\vec{x}_d) \quad (10)$$

$$\nabla_d^2 G(\vec{x}_d; \vec{x}) = -k^2 G(\vec{x}_d; \vec{x}) - \delta(\vec{x}_d - \vec{x}) \quad (11)$$

Substitute equations 10 and 11 into equation 9:

$$\begin{aligned} & \int (\phi(\vec{x}_d) [-k^2 G(\vec{x}_d; \vec{x}) - \delta(\vec{x}_d - \vec{x})] \\ & - G(\vec{x}_d; \vec{x}) [-k^2 \phi(\vec{x}_d) + M_i M_j \phi_{,ij}(\vec{x}_d) - B_i \phi_{,i}(\vec{x}_d) - C \phi(\vec{x}_d)]) dV_d \quad (12) \\ & = \int \vec{n}_d [\phi(\vec{x}_d) \nabla_d G(\vec{x}_d; \vec{x}) - G(\vec{x}_d; \vec{x}) \nabla_d \phi(\vec{x}_d)] dS_d \end{aligned}$$

Simplifying,

$$\begin{aligned} & - \int (\phi(\vec{x}_d) \delta(\vec{x}_d - \vec{x}) + G(\vec{x}_d; \vec{x}) [M_i M_j \phi_{,ij}(\vec{x}_d) - B_i \phi_{,i}(\vec{x}_d) - C \phi(\vec{x}_d)]) dV_d \quad (13) \\ & = \int \vec{n}_d [\phi(\vec{x}_d) \nabla_d G(\vec{x}_d; \vec{x}) - G(\vec{x}_d; \vec{x}) \nabla_d \phi(\vec{x}_d)] dS_d \end{aligned}$$

Equation 13 is true for each volume and its bounding surfaces in figure 1. This form accounts for the inhomogeneous media regions via a Fredholm integral of the second kind. Compute the volume integral over region V_0 , and choose $\vec{x} \in V_0$. The dummy variable subscript is replaced by the number corresponding to the volume over which the integration is conducted:

$$\begin{aligned}
\phi(\vec{x}) + \int G(\vec{x}_0; \vec{x}) [M_i M_j \phi_{,ij}(\vec{x}_0) - B_i \phi_{,i}(\vec{x}_0) - C \phi(\vec{x}_0)] dV_0 \\
= - \int \vec{n}_0 [\phi(\vec{x}_0) \nabla_0 G(\vec{x}_0; \vec{x}) - G(\vec{x}_0; \vec{x}) \nabla_0 \phi(\vec{x}_0)] dS_0, \quad \vec{x} \in V_0
\end{aligned} \tag{14}$$

Split the volume integral into two portions:

$$\begin{aligned}
\phi(\vec{x}) + \int G(\vec{x}_1; \vec{x}) [M_i M_j \phi_{,ij}(\vec{x}_1) - B_i \phi_{,i}(\vec{x}_1) - C \phi(\vec{x}_1)] dV_1 \\
+ \int G(\vec{x}_2; \vec{x}) [M_i M_j \phi_{,ij}(\vec{x}_2) - B_i \phi_{,i}(\vec{x}_2) - C \phi(\vec{x}_2)] dV_2 \\
= - \int \vec{n}_0 [\phi(\vec{x}_0) \nabla_0 G(\vec{x}_0; \vec{x}) - G(\vec{x}_0; \vec{x}) \nabla_0 \phi(\vec{x}_0)] dS_0, \quad \vec{x} \in V_0
\end{aligned} \tag{15}$$

We are trying to approximate local variations in the media within the stencil region by computing the discretization for a node inside the square volume (V_1) as a function of the neighboring stencil nodes on the boundary of the square volume (S_1). Variations in the media outside S_1 (ie. in V_2) are not local, and their effects will be taken into account by other stencils, so the volume integral containing their effects may be set to zero without loss of generality:

$$\begin{aligned}
\phi(\vec{x}) + \int G(\vec{x}_1; \vec{x}) [M_i M_j \phi_{,ij}(\vec{x}_1) - B_i \phi_{,i}(\vec{x}_1) - C \phi(\vec{x}_1)] dV_1 \\
= - \int \vec{n}_0 [\phi(\vec{x}_0) \nabla_0 G(\vec{x}_0; \vec{x}) - G(\vec{x}_0; \vec{x}) \nabla_0 \phi(\vec{x}_0)] dS_0, \quad \vec{x} \in V_1
\end{aligned} \tag{16}$$

To simplify the surface integral, consider the integrating equation 13 over V_3 , with

$\vec{x} \in V_1$:

$$\begin{aligned} 0 &+ \int G(\vec{x}_3; \vec{x}) [M_i M_j \phi_{,ij}(\vec{x}_3) - B_i \phi_{,i}(\vec{x}_3) - C\phi(\vec{x}_3)] dV_3 \\ &= - \int \vec{n}_3 [\phi(\vec{x}_3) \nabla_3 G(\vec{x}_3; \vec{x}) - G(\vec{x}_3; \vec{x}) \nabla_3 \phi(\vec{x}_3)] dS_0 \end{aligned} \quad (17)$$

In this formulation, $\phi(\vec{x}_3)$ in the exterior region (V_3) can be chosen to simplify the problem because it is outside the domain of the variable of interest ($\vec{x} \in V_1$). Set the steady flow variation in V_3 to 0 (eliminate the volume integral):

$$0 = - \int \vec{n} [\phi(\vec{x}_3) \nabla_3 G(\vec{x}_3; \vec{x}) - G(\vec{x}_3; \vec{x}) \nabla_3 \phi(\vec{x}_3)] dS_0 \quad (18)$$

The surfaces in equation 16 and equation 18 are identical, and these two independent equations may be summed:

$$\begin{aligned} \phi(\vec{x}) &+ \int G(\vec{x}_1; \vec{x}) [M_i M_j \phi_{,ij}(\vec{x}_1) - B_i \phi_{,i}(\vec{x}_1) - C\phi(\vec{x}_1)] dV_1 \\ &= - \int \vec{n}_0 [\phi(\vec{x}_0) \nabla_0 G(\vec{x}_0; \vec{x}) - G(\vec{x}_0; \vec{x}) \nabla_0 \phi(\vec{x}_0)] dS_0 \\ &- \int \vec{n}_3 [\phi(\vec{x}_3) \nabla_3 G(\vec{x}_3; \vec{x}) - G(\vec{x}_3; \vec{x}) \nabla_3 \phi(\vec{x}_3)] dS_0, \quad \vec{x} \in V_1 \end{aligned} \quad (19)$$

Note that $\vec{n}_0 = -\vec{n}_3$:

$$\begin{aligned}
\phi(\vec{x}) &+ \int G(\vec{x}_1; \vec{x}) [M_i M_j \phi_{,ij}(\vec{x}_1) - B_i \phi_{,i}(\vec{x}_1) - C\phi(\vec{x}_1)] dV_1 \\
&= -\int \vec{n}_0 \{ \phi(\vec{x}_0) \nabla_0 G(\vec{x}_0; \vec{x}) - G(\vec{x}_0; \vec{x}) \nabla_0 \phi(\vec{x}_0) \} dS_0 \\
&+ \int \vec{n}_0 \{ \phi(\vec{x}_3) \nabla_3 G(\vec{x}_3; \vec{x}) - G(\vec{x}_3; \vec{x}) \nabla_3 \phi(\vec{x}_3) \} dS_0, \quad \vec{x} \in V_1
\end{aligned} \tag{20}$$

The acoustic velocity potential $\phi(\vec{x}_0)$ in V_0 is not related to $\phi(\vec{x}_3)$ in V_3 . To highlight this distinction, set $\phi(\vec{x}_3) = \phi_E$ (E for exterior), but use the dummy variable \vec{x}_0 to combine the surface integrals. The infinite space Green's functions are identical for all volumes.

$$\begin{aligned}
\phi(\vec{x}) &+ \int G(\vec{x}_1; \vec{x}) [M_i M_j \phi_{,ij}(\vec{x}_1) - B_i \phi_{,i}(\vec{x}_1) - C\phi(\vec{x}_1)] dV_1 \\
&= \int \vec{n}_0 \{ (\phi_E(\vec{x}_0) - \phi(\vec{x}_0)) \nabla_0 G(\vec{x}_0; \vec{x}) - G(\vec{x}_0; \vec{x}) (\nabla_0 \phi_E(\vec{x}_0) - \nabla_0 \phi(\vec{x}_0)) \} dS_0, \quad \vec{x} \in V_1
\end{aligned} \tag{21}$$

Again, the exterior field problem is separate from the interior, and ϕ_E or $\nabla \phi_E$ may be chosen on S_0 as a boundary condition for the exterior problem. Select $\phi_E = \phi$ on the boundary:

$$\begin{aligned}
\phi(\vec{x}) &+ \int G(\vec{x}_1; \vec{x}) [M_i M_j \phi_{,ij}(\vec{x}_1) - B_i \phi_{,i}(\vec{x}_1) - C\phi(\vec{x}_1)] dV_1 \\
&= \int G(\vec{x}_0; \vec{x}) \vec{n}_0 \{ \nabla_0 \phi(\vec{x}_0) - \nabla_0 \phi_E \} dS_0, \quad \vec{x} \in V_1
\end{aligned} \tag{22}$$

The difference in the normal derivative terms is the strength of a single layer potential, which will be denoted as $\bar{\sigma}$:

$$\begin{aligned} \phi(\bar{x}) + \int G(\bar{x}_1; \bar{x}) [M_x M_y \phi_{,y}(\bar{x}_1) - B_x \phi_{,x}(\bar{x}_1) - C \phi(\bar{x}_1)] dV_1 \\ = \int G(\bar{x}_0; \bar{x}) \bar{\sigma}(\bar{x}_0) dS_0, \quad \bar{x} \in V_1 \end{aligned} \quad (23)$$

To numerically evaluate the integrals, discretize the surface S_0 , as in figure 2.

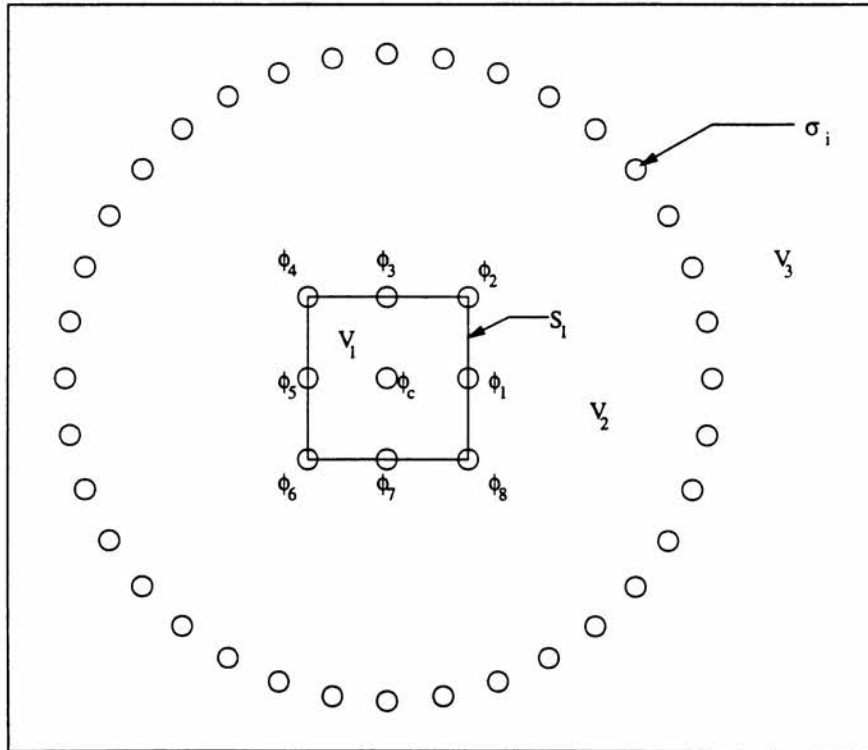


Figure 2. Discretized single layer potential on surface S_0

Approximate the area about each single layer potential node as A_k , and break the volume integral into small blocks of size V_k :

$$\begin{aligned}\phi(\vec{x}) + \sum_k G(\vec{x}_k; \vec{x}) [M_i M_j \phi_{,ij}(\vec{x}_k) - B_i \phi_{,i}(\vec{x}_k) - C \phi(\vec{x}_k)] V_k \\ = \sum_i G(\vec{x}_i; \vec{x}) \bar{\sigma}(\vec{x}_i) A_i\end{aligned}\quad (24)$$

The area A_k can be absorbed into the single layer potential variable. Let $\sigma(\vec{x}_i) = \bar{\sigma}(\vec{x}_i) A_i$:

$$\begin{aligned}\phi(\vec{x}) + \sum_k G(\vec{x}_k; \vec{x}) [M_i M_j \phi_{,ij}(\vec{x}_k) - B_i \phi_{,i}(\vec{x}_k) - C \phi(\vec{x}_k)] V_k \\ = \sum_i G(\vec{x}_i; \vec{x}) \sigma(\vec{x}_i)\end{aligned}\quad (25)$$

Use a summation notation in which all repeated indicies are summed. Note that the spatial vector dependencies are identified by subscripts, that ϕ will be positioned at \vec{x}_j :

$$\phi_j + \tilde{G}_{jk} [M_m M_n \phi_{k'mn} - B_i \phi_{k'i} - C \phi_k] V_k = G_{ji} \sigma_i \quad (26)$$

The acoustic potential ϕ inside the discretized Fredholm volume integral can be approximated by the first order GFD solution for ϕ :

$$\phi_j^{1st\ order} = G_{ji} \sigma_i \quad (27)$$

Implementing this approximation into equation 26:

$$\phi_j + \tilde{G}_{jk}[M_m M_n G_{ki'mn} - B_m G_{ki'm} - CG_{ki}]V_k \sigma_i = G_{ji} \sigma_i \quad (28)$$

$$\phi_j = [G_{ji} + \tilde{G}_{jk}(-M_m M_n G_{ki'mn} + B_m G_{ki'm'm} + CG_{ki})V_k] \sigma_i \quad (29)$$

Combine the Green's function and the discretized Fredholm integral into a single vector:

$$E_{ji} = G_{ji} + \tilde{G}_{jk}(-M_m M_n G_{ki'mn} + B_m G_{ki'm'm} + CG_{ki})V_k \quad (30)$$

E_{ji} represents a corrected Green's function.

Following the normal GFD procedure [4] using this new function, in which the interpolated node at \bar{x}_c ($\bar{x}_c \in V_1$) is determined as a function of its stencil neighbors at locations \bar{x}_j ($j=1, \#$ of stencil neighbors) on S_1 , and using i σ 's on surface S_0 (see figure 2):

$$\begin{aligned} \phi_j &= E_{ji} \sigma_i \\ \phi_c &= E_{ci} \sigma_i \end{aligned} \quad (31)$$

To model a smooth function of σ on surface S_0 , choose $i > j$. Find the least-norm least-squares solution for σ_i by computing the pseudo-inverse of E_{ji} using singular value decomposition (SVD):

$$\begin{aligned}\sigma_i &= E_{ij}^+ \phi_j \\ \phi_c &= E_{ci} E_{ij}^+ \phi_j\end{aligned}\tag{32}$$

The volume integrals need to be evaluated only over the domain of the local computational stencil. In 1-D, these integrals can often be analytically computed if a functional form for the variation is given, while 2-D and 3-D computations require that the volume integral be computed numerically. The Fredholm integral's Green's function must be the correctly weighted free field Green's function, because it has local integrable singularities that have a significant effect on the overall integration. In contrast, the Green's function associated with the 1st order solution can be a locally valid function that satisfies the homogeneous PDE, such as a plane wave or non-singular Bessel function.

While it should be noted that it is possible to analytically extend this method to higher order approximations in 1-D, it is the purpose of this dissertation to identify options that work in multiple dimensions. In addition, this particular Fredholm integral formulation is not desirable for solving general aero-acoustics problems, especially for situations in which the Mach number cannot be considered a perturbation. If the AVPE is spatially transformed back into the Helmholtz equation, then *variations* in $M_i M_j$ and B_i across the stencil can be presumed to be perturbations, instead of assuming $M_i M_j$ and B_i

to be perturbations. Nevertheless, the current formulation does provides improved results for perturbations to the frequency parameter (k), and thus is useful for determining the accuracy of other methods.

2.2. Second Order Perturbation Expansion Method

Local plane wave solutions were used in [7] to obtain a first order accurate solution to equation 3. The approach is extended here to second order by finding particular solutions to the second order equations of the formal perturbation expansion.

The acoustic potential will be expanded as the sum of the first order constant coefficient acoustic potential (ϕ^0) which includes constant flow gradient terms, plus terms of higher order:

$$\phi = \phi^0 + \varepsilon\phi^1 + \varepsilon^2\phi^2 + \dots \quad (33)$$

The variable coefficient acoustic velocity potential equation is rewritten in the form,

$$\begin{aligned} [\delta_{ij} - M_i M_j] \phi_{,ij} + B_i \phi_{,i} + K^2 \phi &= 0 \\ B_i &= -2[M_j M_{i,j} + iM_i k] \\ K^2 &= k^2 - iM_j k_{,j} \end{aligned} \quad (34)$$

The AVPE's coefficients will be expressed as a constant plus a spatially varying part. The constant coefficient terms are the values of the variable coefficients at the location of the node to be discretized (at location \bar{x}_0), while the varying portion is zero at the discretized node:

$$\begin{aligned}
M_i M_j &= (M_i M_j)^0(\bar{x}_0) + \varepsilon (M_i M_j)^1(\bar{x}) \\
B_i &= B_i^0(\bar{x}_0) + \varepsilon B_i^1(\bar{x}) \\
K^2 &= (K^2)^0(\bar{x}_0) + \varepsilon (K^2)^1(\bar{x})
\end{aligned} \tag{35}$$

Substituting these terms into equation 34, and collecting like sums in terms of ε yields (see Appendix B for the complete derivation):

$$[\delta_{ij} - (M_i M_j)^0] \phi^0_{,ij} + B_i^0 \phi^0_{,i} + (K^2)^0 \phi^0 = 0 \tag{36}$$

$$\begin{aligned}
&[\delta_{ij} - (M_i M_j)^0] \phi^n_{,ij} + B_i^0 \phi^n_{,i} + (K^2)^0 \phi^n \\
&= (M_i M_j)^1 \phi^{n-1}_{,ij} - B_i^1 \phi^{n-1}_{,i} - (K^2)^1 \phi^{n-1}
\end{aligned} \tag{37}$$

As solutions to the first equation have already been presented in [7], corrections using the second equation will be sought, with $n=1$. One exact solution to equation 36 is:

$$\phi^0(x_i) = c_k e^{-i q_k x_i}, \quad i = 1-3, \quad k = 1-\infty \tag{38}$$

$$q_{ki} = \frac{v_{kj}B_j + \sqrt{4K^2(1 - (v_{kj}M_j)^2) - (v_{kj}B_j)^2}}{2(1 - (v_{kj}M_j)^2)}v_{ki}, \text{ no sum on } k \quad (39)$$

The unit vector v_{kj} is rotated k times to simulate the asymptotic effect of a surface of free field Green's functions from a great distance. Substitute this exact solution to the constant coefficient solution into the right hand side of equation 37 ($n=1$):

$$\begin{aligned} & [\delta_{ij} - (M_r M_j)^0] \phi^1_{,ij} + B_i^0 \phi^1_{,i} + (K^2)^0 \phi^1 \\ & = [-(M_r M_j)^1 q_{ki} q_{kj} + i q_{ki} B_i^1 - (K^2)^1] c_k e^{-i q_{ki} x_i}, \end{aligned} \quad (40)$$

no sum on } k

The term in brackets is a scalar quantity for each k , and varies in value across the stencil from 0 at the interpolated node. It is possible to express this quantity as a spatial polynomial function, $P(x_i)$.

$$[\delta_{ij} - (M_r M_j)^0] \phi^1_{,ij} + B_i^0 \phi^1_{,i} + (K^2)^0 \phi^1 = P(q_{ki} x_i) c_k e^{-i q_{ki} x_i} \quad (41)$$

A particular solution to account for the right-hand side's polynomial-exponential function shall be sought in the form:

$$\phi^1 = R(q_{ki} x_i) c_k e^{-i q_{ki} x_i} \quad (42)$$

Note that the left hand side of equation 41's homogeneous solution for ϕ^1 is the same as for ϕ^0 . This implies that if P 's highest order polynomial term is n , R will have

to contain polynomial terms of order $n+1$. Once P is selected, the R 's polynomial coefficients will be determined by the method of undetermined coefficients.

The form of P is arbitrary, and two means of computing the polynomial have been examined:

- 1) An n -dimensional quadratic Lagrangian polynomial is used to generate a continuous function that takes into account the flow field at each stencil node.
- 2) The 2nd order steady flow terms are approximated by a Taylor series expansion centered at the interpolated node.

The former method guarantees a function that takes the flow variation into account across the stencil. However, in 2-D the resulting P polynomial does contain 3rd order polynomial terms, requiring 4th order polynomial terms in R . In Chapter 3 (Implementation and Results), it will be demonstrated that the Taylor Series method, using 2nd order terms in P , has the same accuracy as quadratic Lagrangian interpolation, even though it only requires 3rd order polynomial terms in R . Reducing the order of the polynomial also reduces the computational effort required to solve for the undetermined coefficients, which is especially important for 3-D problems. The 1-D, 2-D and 3-D Taylor series correction factors are derived in this chapter, and the 2-D quadratic Lagrangian quadratic correction factors are derived in Appendix C.

Proceeding with the general process used to determine the correction coefficients, it is necessary to substitute the assumed form of the particular solution into the PDE, and

collect like derivative terms of the R polynomial. The derivatives of the particular solution are of the form:

$$\begin{aligned}
\phi^1 &= c_k R e^{-iq_k x_i} \\
\phi_{,i}^1 &= c_k (R_{,i} - iq_{ki} R) e^{-iq_k x_i} \\
\phi_{,ij}^1 &= c_k (R_{,ij} - iq_{ki} R_{,j} - iq_{kj} R_{,i} - q_{ki} q_{kj} R) e^{-iq_k x_i} \\
\phi_{,ii}^1 &= c_k (R_{,ii} - 2iq_{ki} R_{,i} - q_{ki}^2 R) e^{-iq_k x_i}
\end{aligned} \tag{43}$$

Expanding this in 3-D:

$$\begin{aligned}
\phi^1 &= c_k R e^{-iq_k x_i} \\
\phi_{,x}^1 &= c_k (R_{,x} - iq_{kx} R) e^{-iq_k x_i} \\
\phi_{,y}^1 &= c_k (R_{,y} - iq_{ky} R) e^{-iq_k x_i} \\
\phi_{,z}^1 &= c_k (R_{,z} - iq_{kz} R) e^{-iq_k x_i} \\
\phi_{,xy}^1 &= c_k (R_{,xy} - iq_{kx} R_{,y} - iq_{ky} R_{,x} - q_{kx} q_{ky} R) e^{-iq_k x_i} \\
\phi_{,xz}^1 &= c_k (R_{,xz} - iq_{kx} R_{,z} - iq_{kz} R_{,x} - q_{kx} q_{kz} R) e^{-iq_k x_i} \\
\phi_{,yz}^1 &= c_k (R_{,yz} - iq_{ky} R_{,z} - iq_{kz} R_{,y} - q_{ky} q_{kz} R) e^{-iq_k x_i} \\
\phi_{,xx}^1 &= c_k (R_{,xx} - 2iq_{kx} R_{,x} - q_{kx}^2 R) e^{-iq_k x_i} \\
\phi_{,yy}^1 &= c_k (R_{,yy} - 2iq_{ky} R_{,y} - q_{ky}^2 R) e^{-iq_k x_i} \\
\phi_{,zz}^1 &= c_k (R_{,zz} - 2iq_{kz} R_{,z} - q_{kz}^2 R) e^{-iq_k x_i}
\end{aligned} \tag{44}$$

Restate the constant-coefficient left hand side of the PDE as:

$$\begin{aligned}
 & A\phi^1 + B\phi_{,x}^1 + C\phi_{,xx}^1 + D\phi_{,xy}^1 + E\phi_{,y}^1 + F\phi_{,yy}^1 \\
 & + G\phi_{,xz}^1 + H\phi_{,yz}^1 + I\phi_{,z}^1 + J\phi_{,zz}^1 = Pc_k e^{-iq_k x_i}
 \end{aligned} \tag{45}$$

To assist in solving the system of undetermined coefficients, substitute the assumed particular solution into the PDE, cancel the $c_k e^{-iq_k x_i}$ terms and collect like terms of R:

	R	$R_{,x}$	$R_{,xx}$	$R_{,xy}$	$R_{,y}$	$R_{,yy}$	$R_{,xz}$	$R_{,yz}$	$R_{,z}$	$R_{,zz}$
$A\phi^1$	A									
$B\phi_{,x}^1$	$-iq_{kx}B$	B								
$C\phi_{,xx}^1$	$-q_{kx}^2C$	$-2iq_{kx}C$	C							
$D\phi_{,xy}^1$	$-q_{kx}q_{ky}D$	$-iq_{ky}D$		D	$-iq_{kx}D$					
$E\phi_{,y}^1$	$-iq_{ky}E$				E					
$F\phi_{,yy}^1$	$-q_{ky}^2F$				$-2iq_{ky}F$	F				
$G\phi_{,xz}^1$	$-q_{kx}q_{kz}G$	$-iq_{kz}G$					G	$-iq_{kx}G$		
$H\phi_{,yz}^1$	$-q_{ky}q_{kz}H$				$-iq_{kz}H$		H	$-iq_{ky}H$		
$I\phi_{,z}^1$	$-iq_{kz}I$							I		
$J\phi_{,zz}^1$	$-q_{kz}^2J$						$-2iq_{kz}J$	J		

The terms in the first column sum to zero, as these coefficients represent the homogeneous solution being substituted into the PDE. Summing the columns,

$$\begin{array}{rcl}
& 1-D & 2-D & 3-D \\
a_1 R_x & = (B - i2q_k C & - iq_k D & - iq_k G) R_x \\
a_2 R_{xx} & = CR_{xx} & & \\
a_3 R_y & = & (-iq_k D + E - 2iq_k F & - iq_k H) R_y \\
a_4 R_{yy} & = & FR_{yy} & \\
a_5 R_z & = & & (-iq_k G - iq_k H + I - 2iq_k J) R_z \\
a_6 R_{zz} & = & & JR_{zz} \\
a_7 R_{xy} & = & DR_{xy} & \\
a_8 R_{xz} & = & & GR_{xz} \\
a_9 R_{yz} & = & & HR_{yz}
\end{array} \tag{47}$$

This chart is useful for determining the coefficients required in solving for R's undetermined coefficients in 1, 2 and 3-D.

In the 1-D case, choose $P = p_1 x + p_2 x^2$, as would be required using either quadratic Lagrangian interpolation or a 2nd order Taylor series. Correspondingly, choose $R = [r_1 x, r_2 x^2, r_3 x^3]$. Then,

$$\begin{aligned}
a_1 R_x &= a_1 [1, 2x, 3x^2] \cdot \bar{r} \\
a_2 R_{xx} &= a_2 [0, 2, 6x] \cdot \bar{r}
\end{aligned} \tag{48}$$

$$\begin{bmatrix} a_1 & 2a_2 & 0 \\ 0 & 2a_1 & 6a_2 \\ 0 & 0 & 3a_1 \end{bmatrix} \begin{bmatrix} r_1 \\ r_2 \\ r_3 \end{bmatrix} = \begin{bmatrix} 0 \text{ (constant row)} \\ p_1 \text{ (x row)} \\ p_2 \text{ (x}^2 \text{ row)} \end{bmatrix} \tag{49}$$

This system of equations can be solved for \vec{r} . This information is then used by computing the second order terms and adding them to the first order terms:

$$\phi^1 = [x, x^2, x^3] \cdot \vec{r}(q_{kl}) c_k e^{-iq_{kl}x_i} \quad (50)$$

$$\begin{aligned} \phi &= \phi^0 + \epsilon \phi^1 \\ &= (1 + \epsilon [x, x^2, x^3] \cdot \vec{r}(q_{kl}) c_k e^{-iq_{kl}x_i}) \end{aligned} \quad (51)$$

This corrected function (notably *not* the free field Green's function) is then used to compute the discretization.

In two dimensions, again assume that P will represent a 2nd order Taylor's series expansion of the varying flow field parameters:

$$P = [x, x^2, xy, y, y^2] \cdot \vec{p} \quad (52)$$

Choose R to be of the form:

$$R = [x^2, y^2, x^3, x^2y, xy^2, y^3] \cdot \vec{r} \quad (53)$$

Taking the spatial derivatives of R,

$$a_1 R_x = [2x, 0, 3x^2, 2xy, y^2, 0] \cdot \vec{r} \quad (54)$$

Taylor series only requires 3rd order polynomial terms. One set of terms that yields a linearly independent set of equations for all direction vectors (q_{ki}) is:

$$R(x,y,z,q_{ki}) = \bar{r}(x^2, y^2, z^2, x^3, x^2y, x^2z, xy^2, xyz, xz^2, y^3, y^2z, yz^2, z^3) \quad (60)$$

The system of equations to solve for \bar{r} is:

$$\begin{bmatrix} 2a_2 & 2a_4 & 2a_6 \\ 2a_1 & & 6a_2 & 2a_7 & 2a_8 & 2a_4 & a_9 & 2a_6 \\ & 2a_3 & & 2a_2 & & 2a_7 & a_8 & & 6a_4 & 2a_9 & 2a_6 \\ & & 2a_5 & & 2a_2 & & a_7 & 2a_8 & & 2a_4 & 2a_9 & 6a_6 \\ & & & 3a_1 & a_3 & a_5 & & & & & & & \\ & & & & 2a_1 & & 2a_3 & a_5 & & & & & \\ & & & & & 2a_1 & & a_3 & 2a_5 & & & & \\ & & & & & & a_1 & & a_3 & a_5 & & & \\ & & & & & & & a_1 & & 2a_3 & 2a_5 & & \\ & & & & & & & & a_1 & & a_3 & 3a_5 & \end{bmatrix} \begin{bmatrix} r_1 \\ r_2 \\ r_3 \\ r_4 \\ r_5 \\ r_6 \\ r_7 \\ r_8 \\ r_9 \\ r_{10} \\ r_{11} \\ r_{12} \\ r_{13} \end{bmatrix} = \begin{bmatrix} 0 \text{ (constant row)} \\ p_1 \text{ (x row)} \\ p_2 \text{ (y row)} \\ p_3 \text{ (z row)} \\ p_4 \text{ (x}^2 \text{ row)} \\ p_5 \text{ (xy row)} \\ p_6 \text{ (xz row)} \\ p_7 \text{ (y}^2 \text{ row)} \\ p_8 \text{ (yz row)} \\ p_9 \text{ (z}^2 \text{ row)} \end{bmatrix} \quad (61)$$

Note that this system of equations is under-constrained; there are 13 unknowns (\bar{r}) and only 10 equations. If any of the \bar{r} terms are removed, the system of equations will not be linearly independent for certain direction vectors, as some of the a_i parameters are functions of q_{ki} . We can resort to SVD to determine the least-norm least-squares \bar{r} , or we can impose three artificial constraints to create a unique solution for \bar{r} . The implementation of this 3-D formulation is a part of ongoing research.

CHAPTER 3

IMPLEMENTATION AND RESULTS

The criteria defining the success of the Green's function correction factors for inhomogeneous media is whether or not any improvement in accuracy over previous methods can be demonstrated, and if so, how much extra effort is required to compute the correction factors.

3.1. Description of Tests Performed

Several test cases have been examined to determine how well these correction factors improve GFD's accuracy in computational domains with inhomogeneous media. To simplify the analysis, only the frequency parameter $(K^2)^1$ is varied across the computational domain. Variations due to the Mach number appear in the right hand side of equation 40 as directionally dependent variations in the frequency:

$$-(M_i M_j)^1 q_{ki} q_{kj} + i q_{ki} B_i^1 - (K^2)^1 \quad (62)$$

Examining the variation in $(K^2)^1$ should be sufficient to analyze the methods' accuracies. Varying $(K^2)^1$ is analogous to allowing the speed of sound (c) or the temperature to vary across the computational stencil.

Two different kinds of meshes are used in the evaluation: a 1-D eleven node mesh and a 2-D 15x15 node mesh. In 1-D, the square of the reduced frequency is varied linearly, while in 2-D, a Bessel function "bump" in the square of the frequency is centered in the middle of the domain. Both the 1-D and 2-D cases assume an incoming plane wave as one boundary condition, and allow the wave to interact with the inhomogeneity. The scattered wave is allowed to radiate from the computational domain in all directions. It should be noted that the acoustic medium is assumed to be homogeneous at all the boundaries.

3.2. Explanation of Error Plots

The accuracy of the method is determined by comparing the computed solution for the acoustic potential (ϕ) with a numerically computed "pseudo-exact" solution. The pseudo-exact solutions are computed on a denser mesh using the Fredholm integral formulation in 1-D (100x denser mesh), and the 2nd order Taylor series perturbation expansion in 2-D (10x denser mesh in each dimension).

The acoustic potential is a complex number, and can be expressed as $re^{i\theta}$. To determine the accuracy of the amplitude, r , the error is computed as:

$$Error_{amplitude} = \frac{|r - r_{exact}|}{r_{exact}} \quad (63)$$

Similarly, the error in the phase (θ) is computed as

$$Error_{phase} = \frac{1}{2\pi} \begin{cases} |\theta - \theta_{Exact}|, & |\theta - \theta_{Exact}| \leq \pi \\ 2\pi - |\theta - \theta_{Exact}|, & |\theta - \theta_{Exact}| > \pi \end{cases}, \quad 0 \leq \theta, \theta_E < 2\pi \quad (64)$$

To simulate varying the mesh density, the reduced frequency parameter k ($= \omega L/c$) is normalized by setting the length parameter equal to the mesh spacing, and the reduced frequency is then varied from near 0 to $\pi/\sqrt{2}$. The effective limit of GFD occurs at the resonant frequency of a stencil, in this case at $\pi/\sqrt{2}$. For each frequency, the amplitude and phase error are computed. The error is then plotted on a log scale versus the frequency. A log scale is needed on the y axis as the errors vary by orders of magnitude over the frequency range.

3.3. 1-D Linearly Varying Reduced Frequency Cases

The computational domain and the corresponding variation in the reduced frequency are presented in figure 3. The frequency is linearly increased using a perturbation parameter H ($k^2 = k_0^2(1 + Hx)$), and in the computations H is set to 0.01, 0.1, and 1.

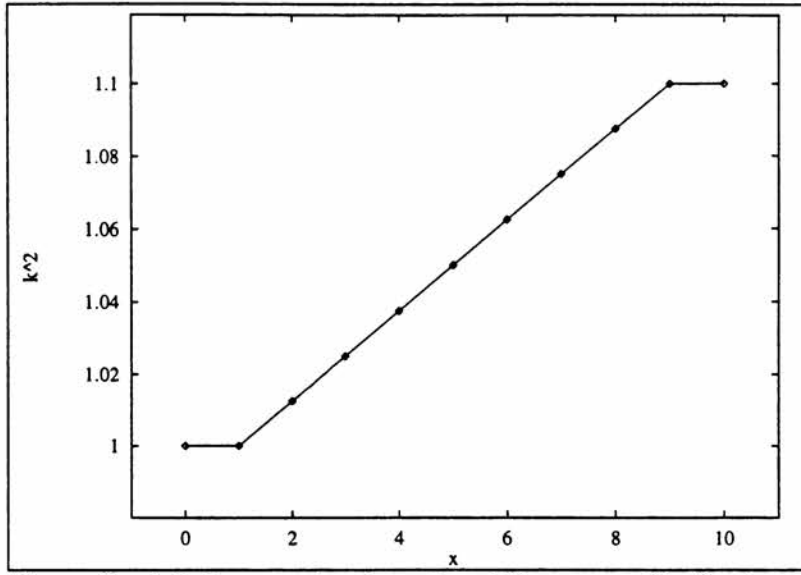


Figure 3. 1-D Computational mesh and frequency distribution

The Fredholm integral is analytically integrated, and takes into account the discontinuity in the derivative at $x=1$ and $x=9$. The homogeneous solutions to the 1-D Helmholtz equation are left and right traveling plane waves:

$$G_R(x, x_0) = e^{-ik(x - x_0)} \quad (65)$$

$$G_L(x, x_0) = e^{ik(x - x_0)}$$

Similarly, the free field Green's function is

$$G(x, x_0) = \frac{1}{2ik} e^{-ik|x - x_0|} \quad (66)$$

For each stencil, the volume integral is separated into two portions to account for the left

and right running waves. The square of the reduced frequency is given to be piecewise linear, so a different linear function is substituted for $(K^2)^1$ in each side of the volume integral.

$$E(\bar{x}_j; \bar{x}_k) = G(\bar{x}_k; \bar{x}_j) + \int G(\bar{x}_0; \bar{x}_j) (K^2)^1 G(\bar{x}_k; \bar{x}_0) dV_0 \quad (67)$$

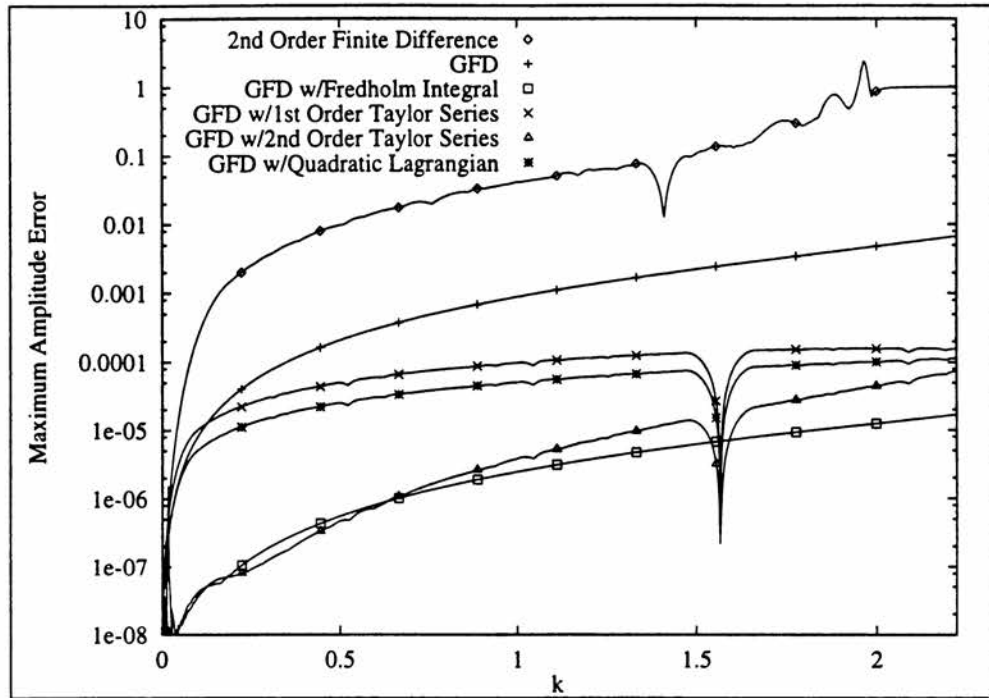
$$(K^2)_L^1 = \alpha x \quad (68)$$

$$(K^2)_R^1 = \beta x$$

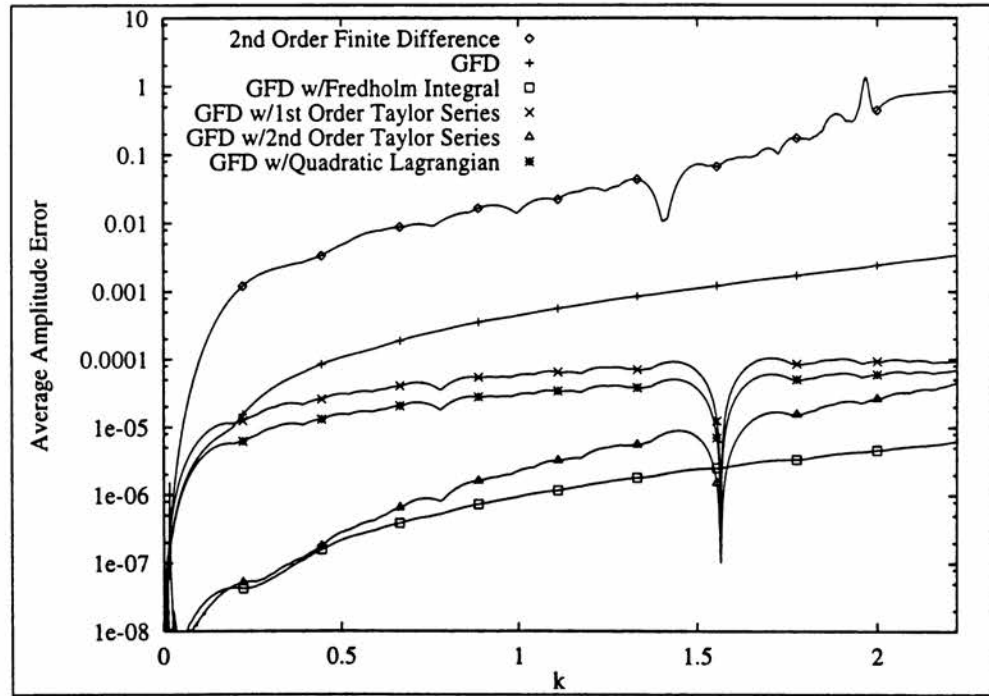
$$E(\bar{x}_j; \bar{x}_k) = \begin{cases} G_L(x_k; x_j) + \int_{x_1}^{x_c} G(x_0; x_j) \alpha x_0 G_L(x_k; x_0) dV_0 + \int_{x_2}^{x_c} G(x_0; x_j) \beta x_0 G_L(x_k; x_0) dV_0, & v_{kl} = 1 \\ G_R(x_k; x_j) + \int_{x_1}^{x_c} G(x_0; x_j) \alpha x_0 G_R(x_k; x_0) dV_0 + \int_{x_2}^{x_c} G(x_0; x_j) \beta x_0 G_R(x_k; x_0) dV_0, & v_{kl} = -1 \end{cases} \quad (69)$$

Both integrals are analytically computed and used as the correction factors for the Fredholm integral cases presented in this section. The second order perturbation expansion cases include a 1st and 2nd order Taylor series expansion, and a quadratic Lagrangian interpolation of the field (the latter two presented in section 2.3).

As figures 4-6 demonstrate, the 2nd order Taylor series and the Fredholm integral corrections significantly improve the accuracy of GFD for inhomogeneous media. Much of the error in the 1st order Taylor series and the quadratic Lagrangian cases, and to some extent the 2nd order Taylor series, is due to the discontinuity in the variation of the frequency near the boundary.

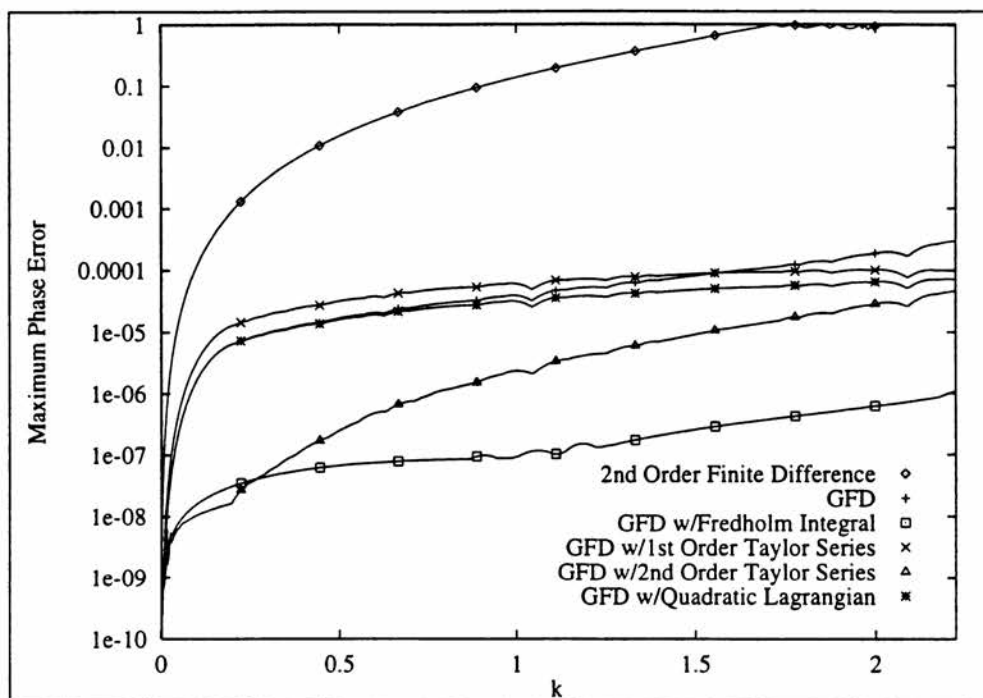


a. maximum amplitude error

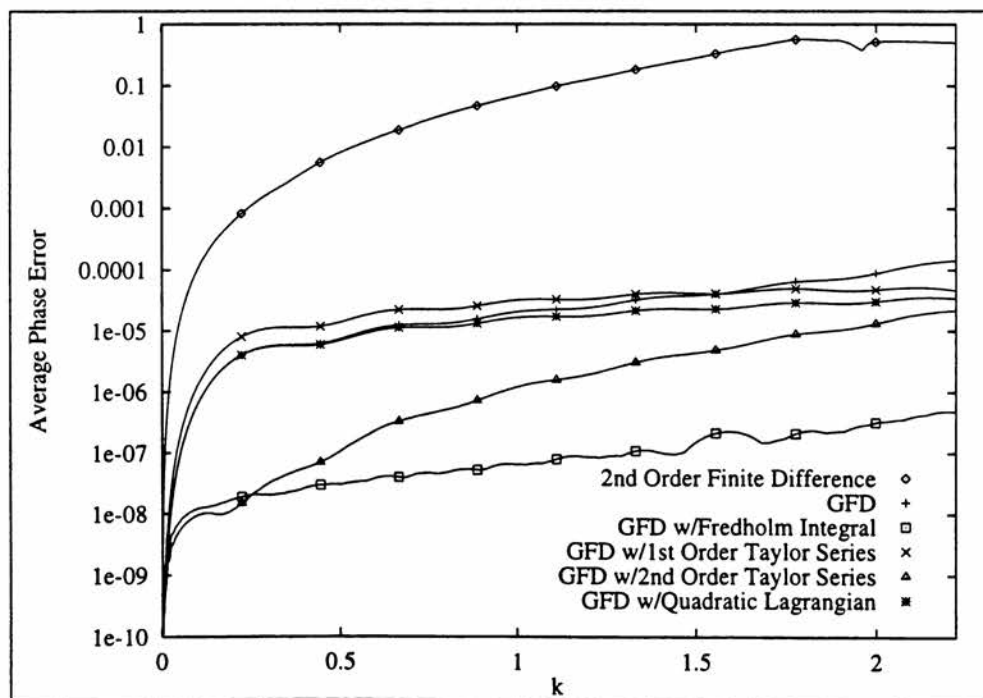


b. average amplitude error

Figure 4. 1-D Method comparison, $H = 0.01$

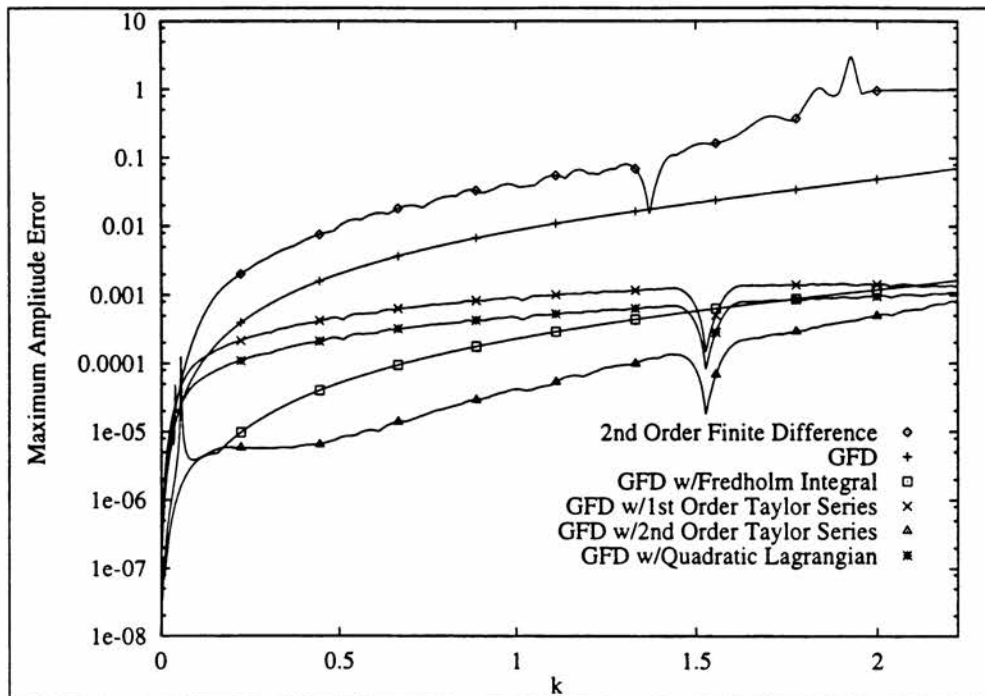


c. maximum phase error

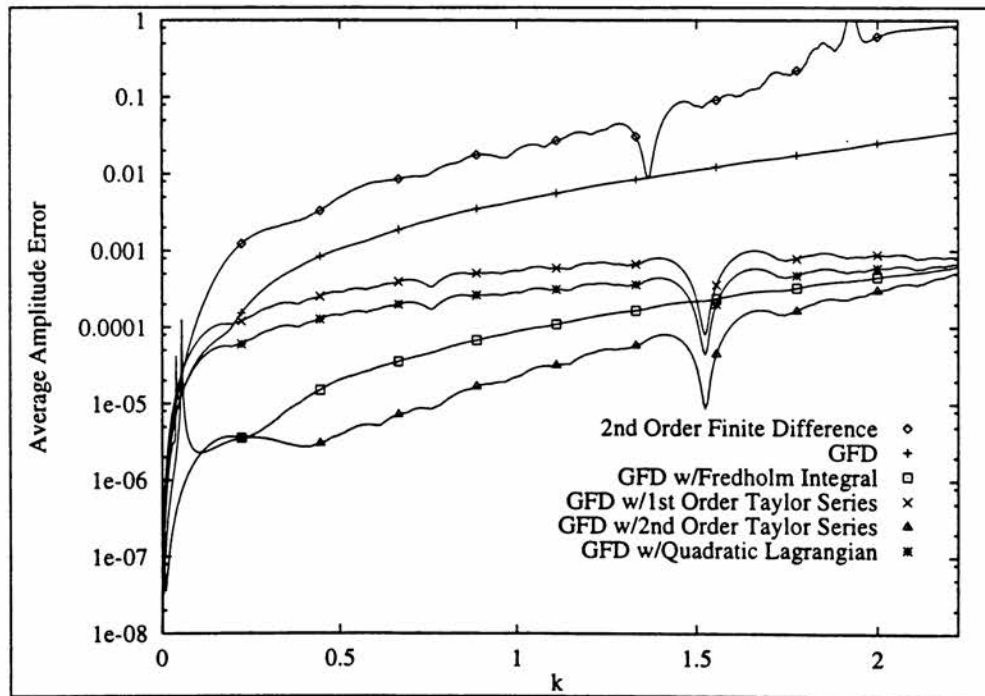


d. average phase error

Figure 4. (continued)

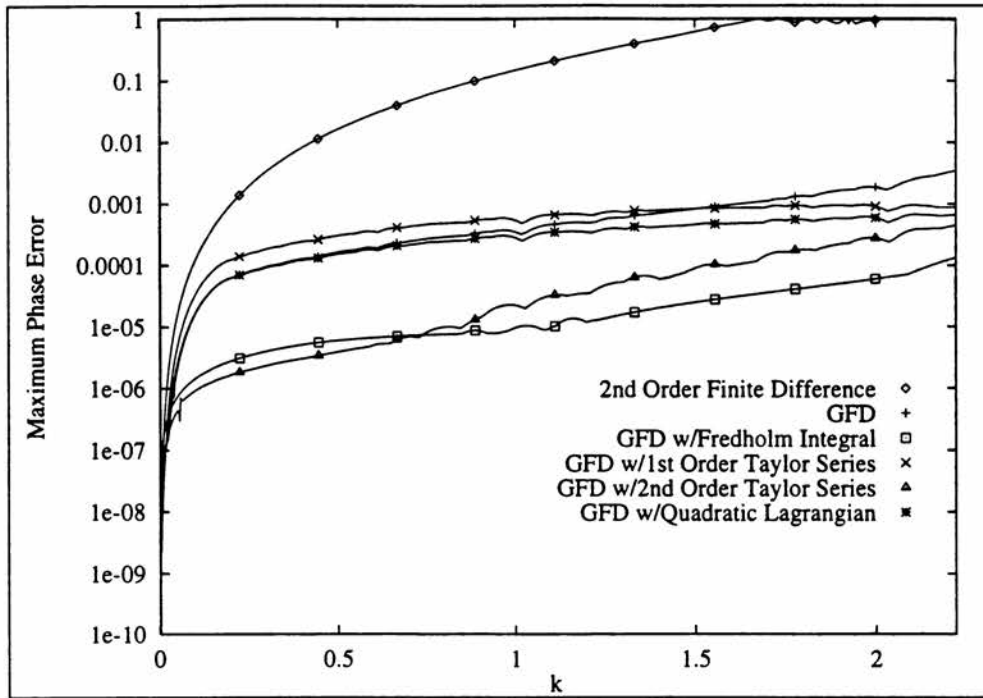


a. maximum amplitude error

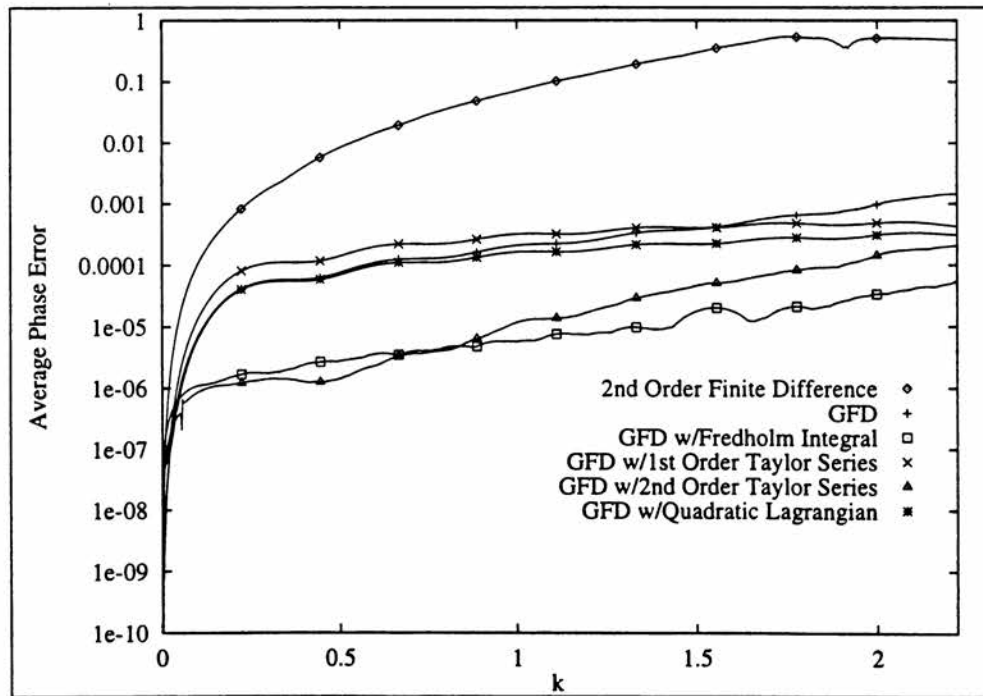


b. average amplitude error

Figure 5. 1-D Method comparison, $H = 0.1$

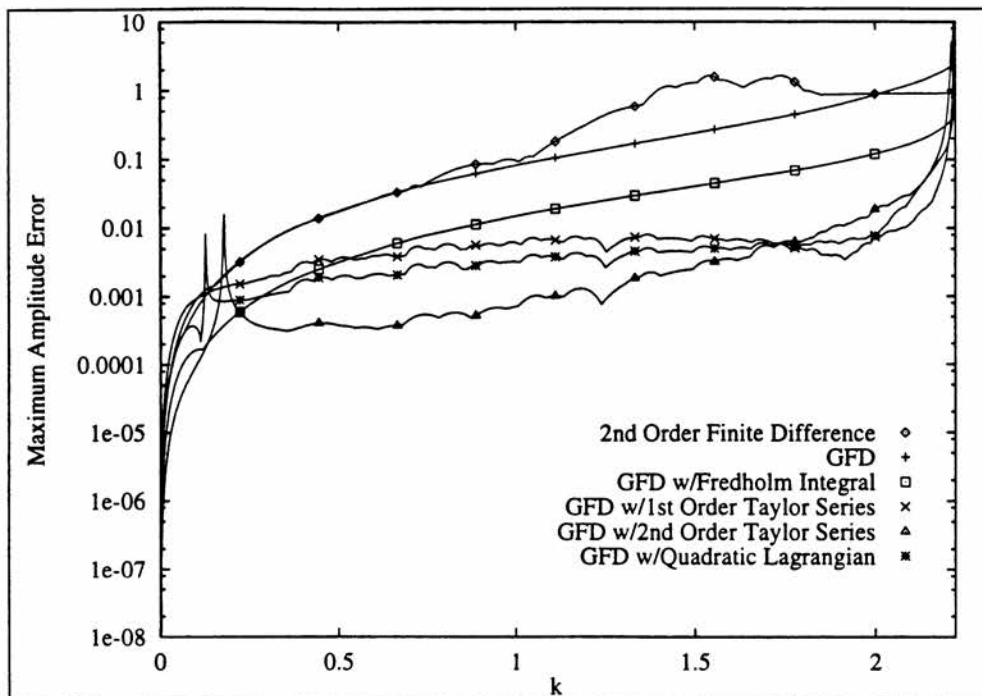


c. maximum phase error

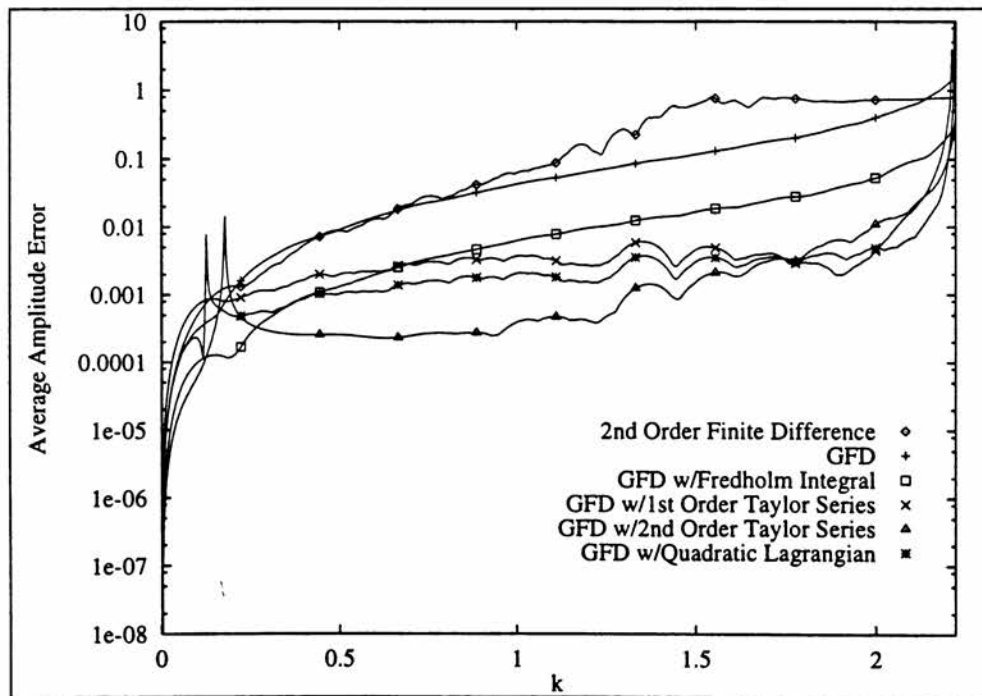


d. average phase error

Figure 5. (continued)

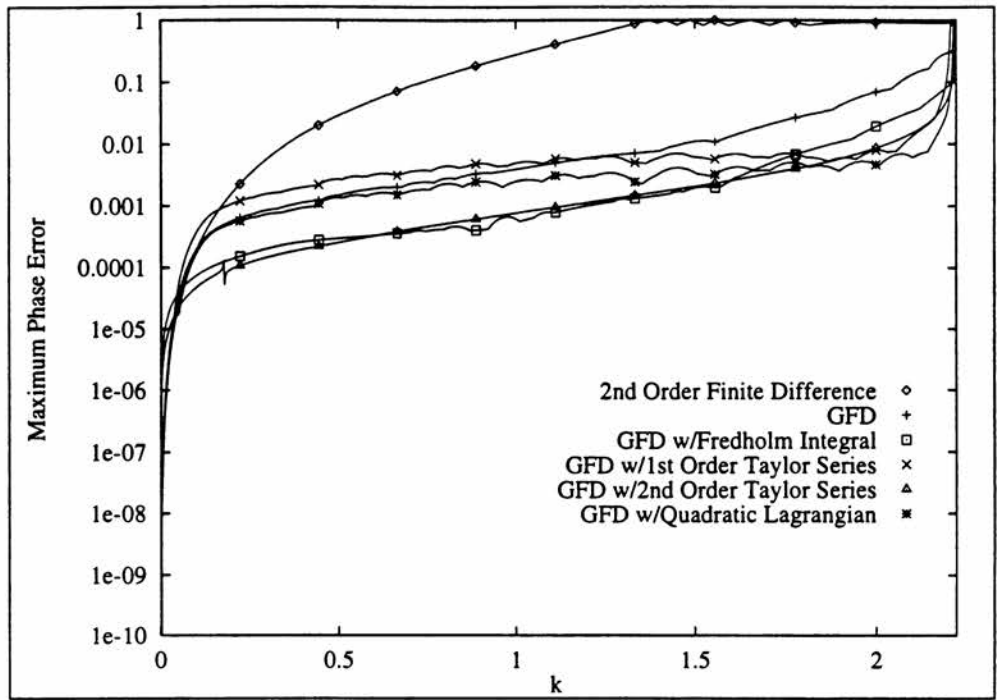


a. maximum amplitude error

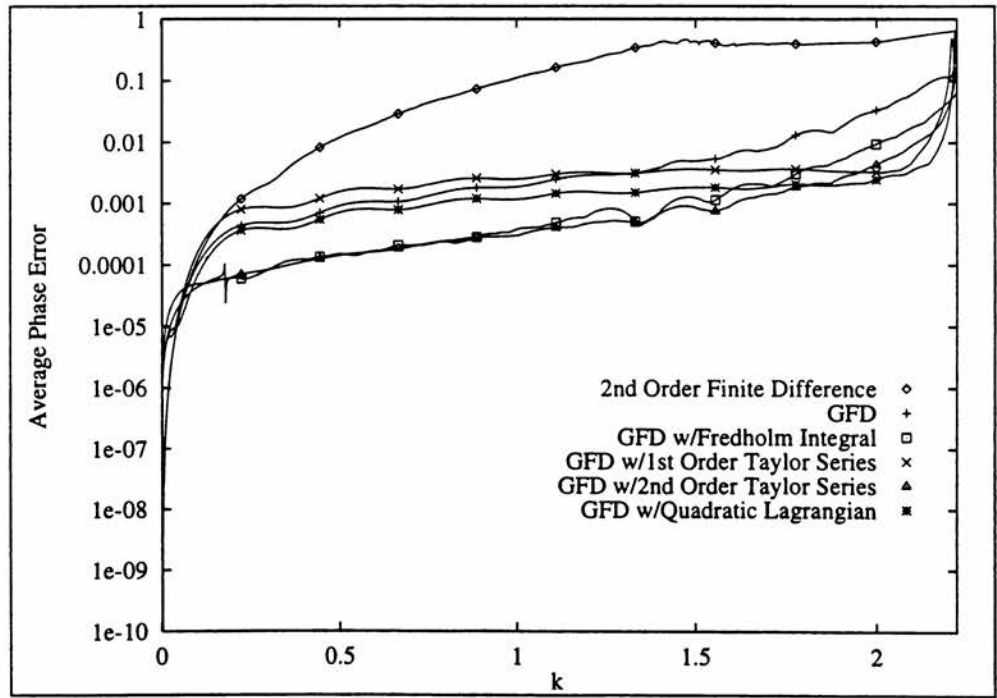


b. average amplitude error

Figure 6. 1-D Method comparison, $H = 1.0$



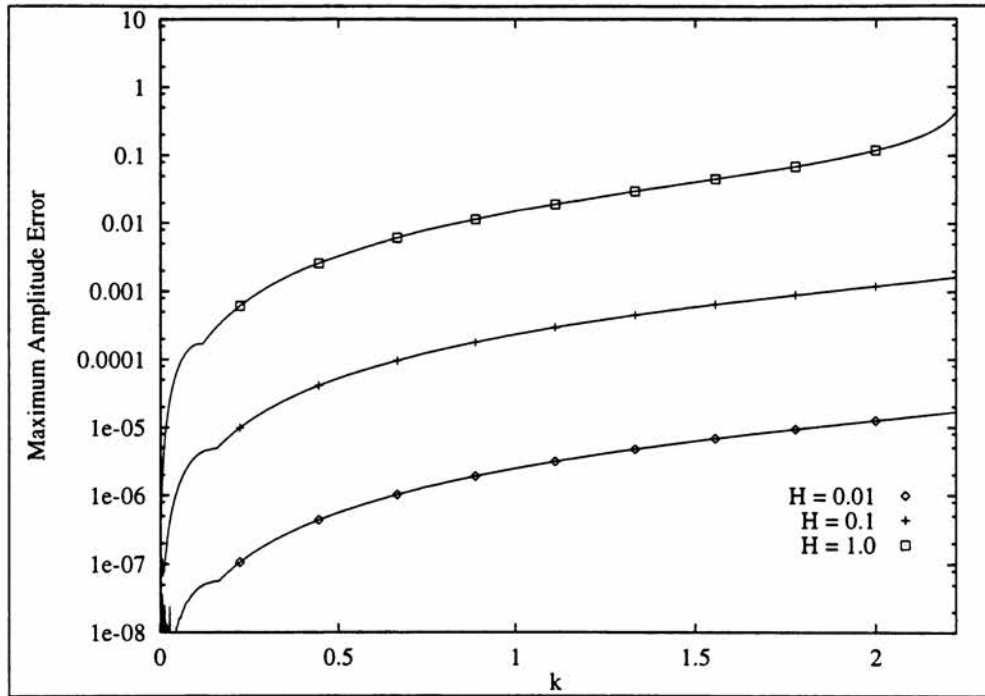
c. maximum phase error



d. average phase error

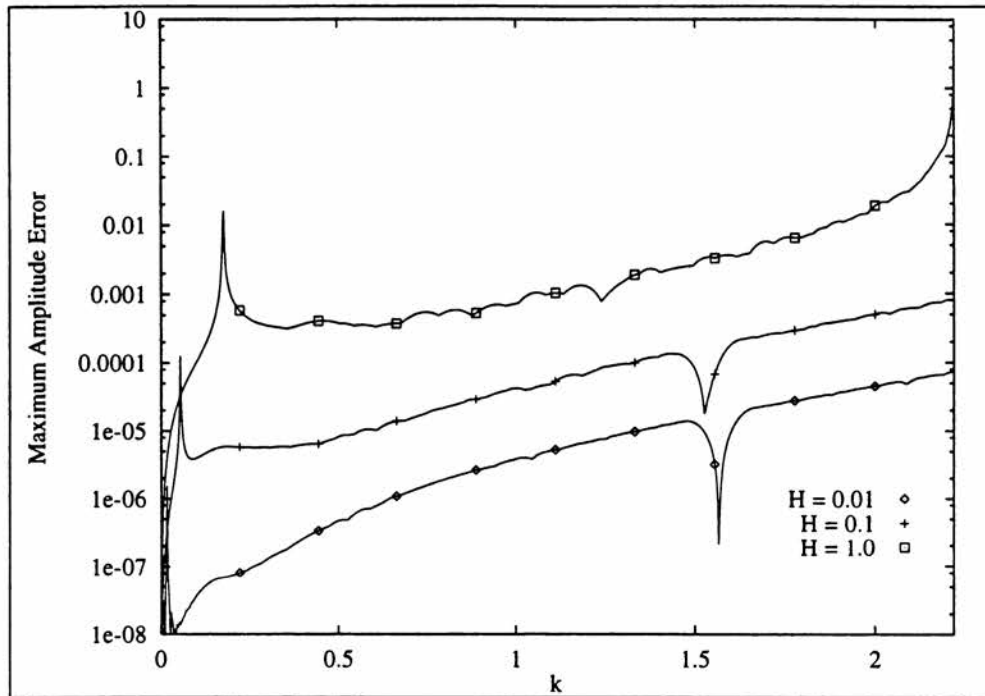
Figure 6. (continued)

Examination of figures 7a and 7b reveals that as the size of the perturbation is decreased, the correction factors become proportionately more accurate. This is to be expected, as the size of the correction factor is a linear function of the size of the perturbation.



a. GFD w/Fredholm integral formulation

Figure 7. 1-D Method comparison for varying values of H



b. GFD w/2nd order Taylor series perturbation expansion

Figure 7. 1-D Method comparison for varying values of H

3.4. 2-D Bessel Function "Bump" Reduced Frequency Cases

The computational domain, a circular inhomogeneous region and an incoming plane wave, are presented in figure 8. The square of the reduced frequency in the inhomogeneous media region follows the shape of a non-singular Bessel function:

$$r = \sqrt{(x-x_c)^2 + (y-y_c)^2}$$

$$\beta = \begin{cases} r, & r \geq R_0 \\ \sqrt{1 + H \frac{J_0(\alpha r/R_0) - J_0(\alpha)}{1 - J_0(\alpha)}}, & r < R_0 \end{cases} \quad (70)$$

$$k_{media} = \beta k$$

The function's parameters are as follows:

R_0 : radius of circular inhomogeneous region

c_x, c_y : center of inhomogeneous region

α : 1st zero of J_1

H : a parameter that varies the height of the "bump"

The Fredholm integral is numerically integrated by dividing the stencil into smaller squares and summing the functional values over the areas. To simplify matters, the homogenous solution is chosen as the Bessel function $J_0(kr)$, which Engels¹ has proven to be an optional choice for σ 's located close to the computational stencil.

The particular solution is computed using both 1st and 2nd order Taylor series (the latter presented in section 2.3), and a quadratic Lagrangian polynomial (see Appendix C). The computational effort to compute the particular solution for the Taylor series is significantly smaller than that required for quadratic Lagrangian interpolation.

Figures 9-11 demonstrate slightly different results in comparison to the 1-D cases. As the field variation is a "bump", second order variation in the field exists, as might be

¹UTSI Engineering Science professor

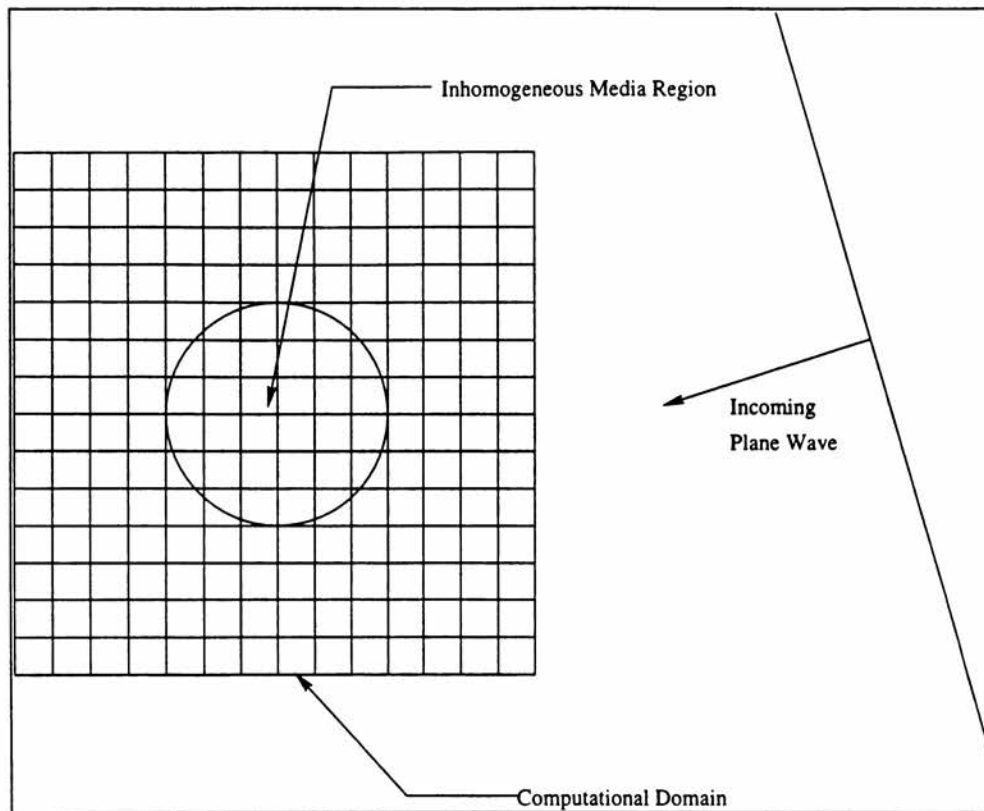
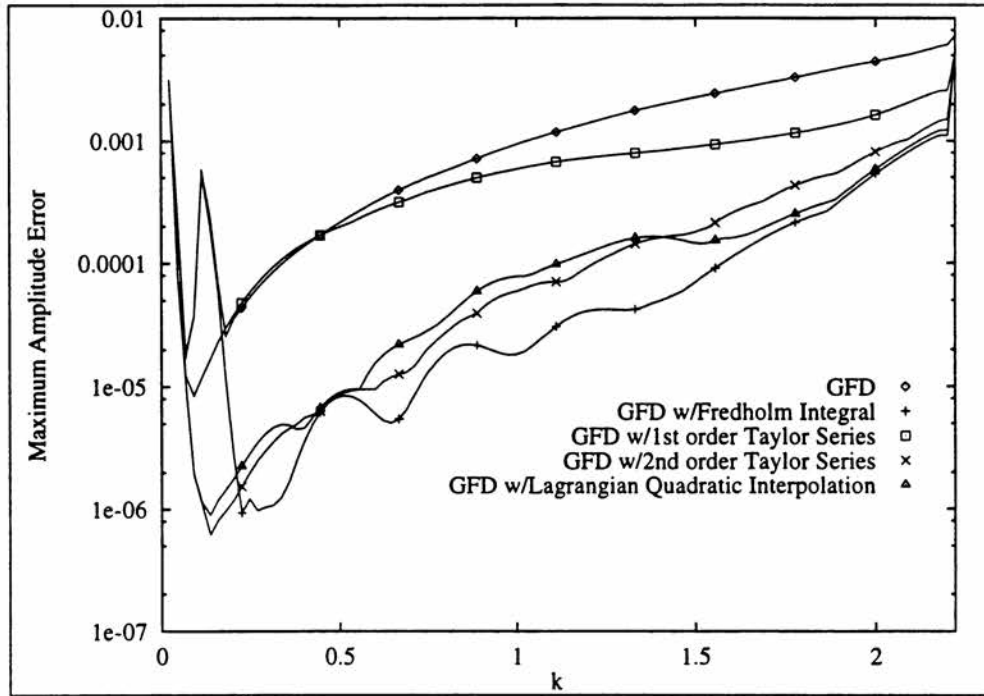
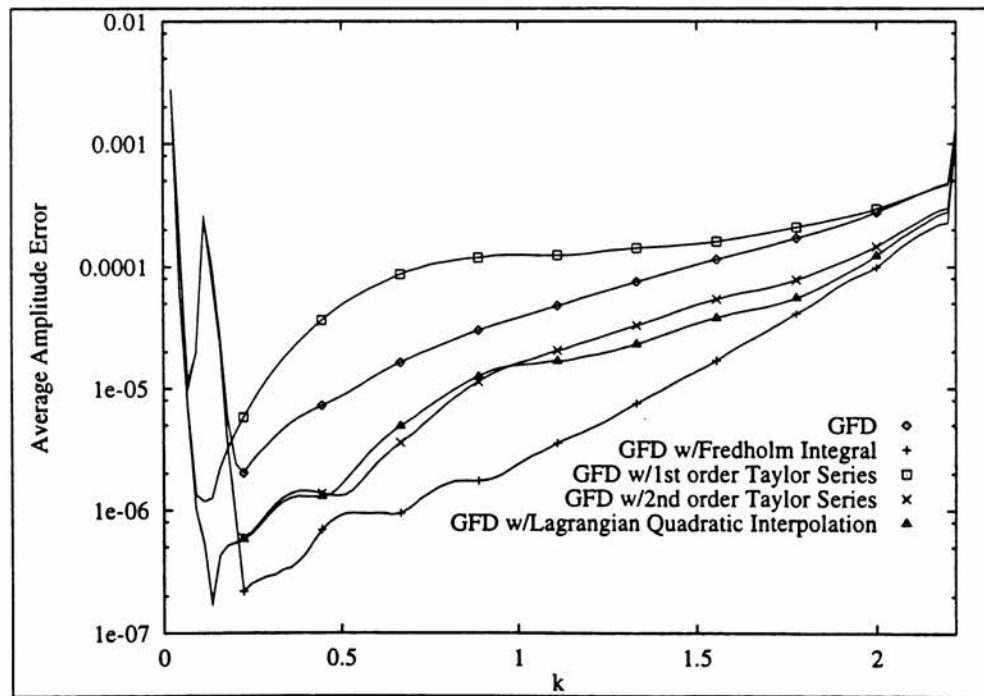


Figure 8b. 2-D Computational mesh and inhomogeneous media region

expected in a real flow field situation. This makes the 1st order Taylor series incapable of accurately correcting the Green's function, and increases the average error results and the maximum phase errors. The Fredholm integral method's accuracy is greatly affected by the size of the perturbation (H), and decreases in accuracy from a perturbation with $H=0.01$ (figure 9a) to a perturbation with $H=1$ (figure 11a). In contrast, in 2-D the 2nd order Taylor series and quadratic Lagrangian interpolation methods remain relatively constant with respect to perturbation size.

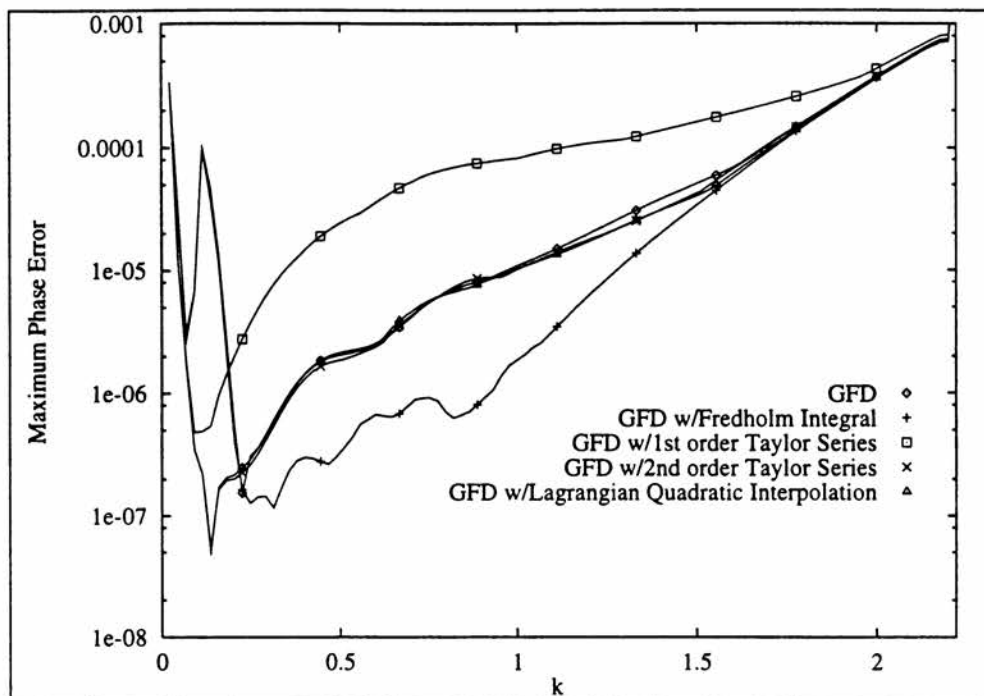


a. maximum amplitude error

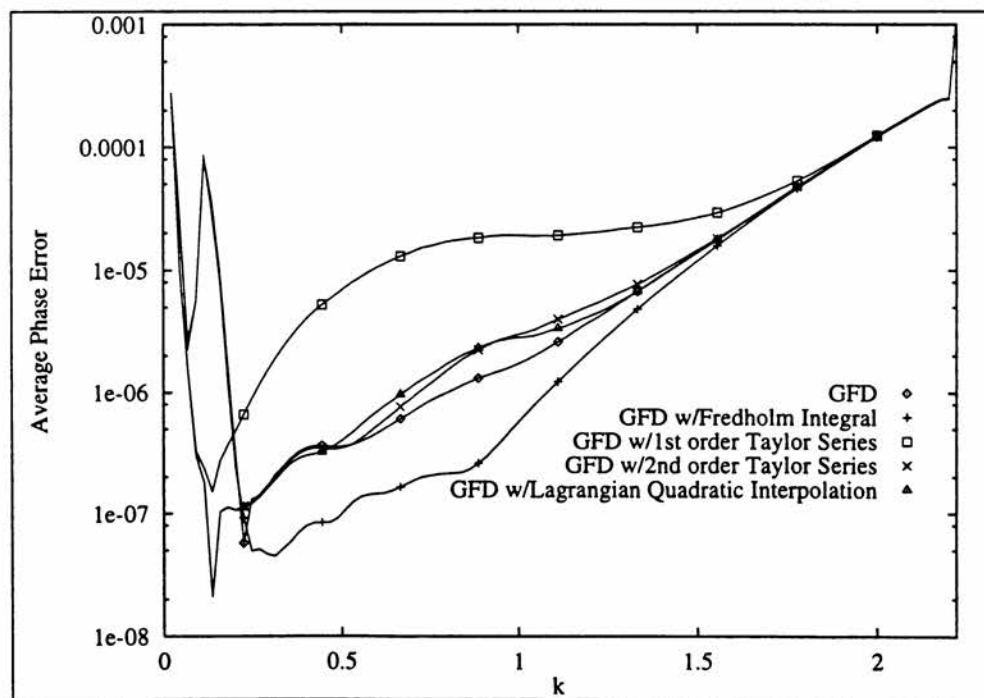


b. average amplitude error

Figure 9. 2-D Method comparison, $H = 0.01$

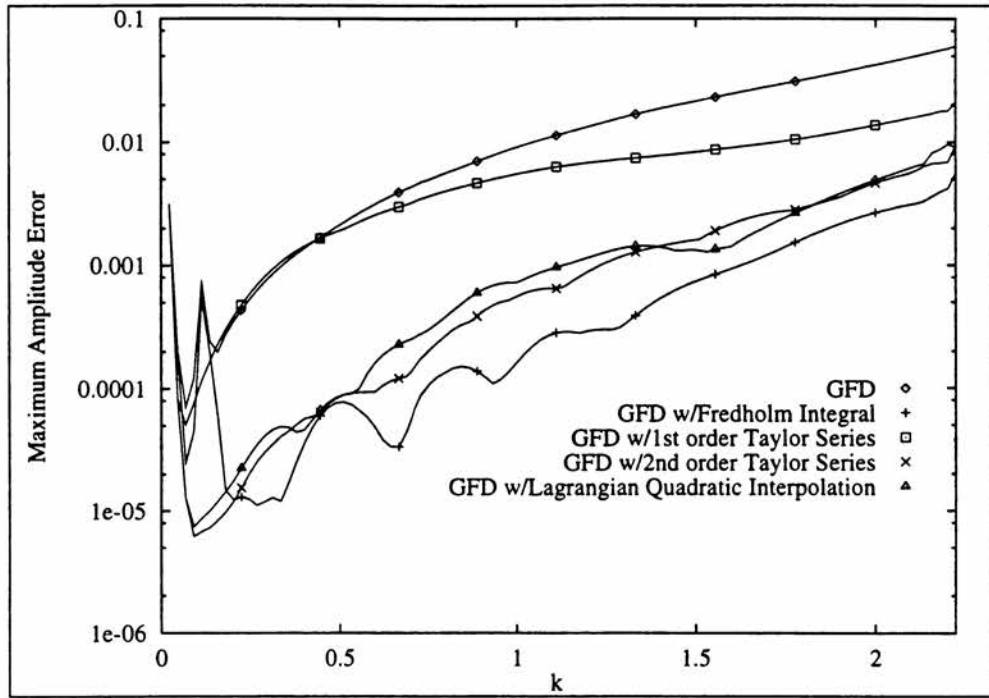


c. maximum phase error

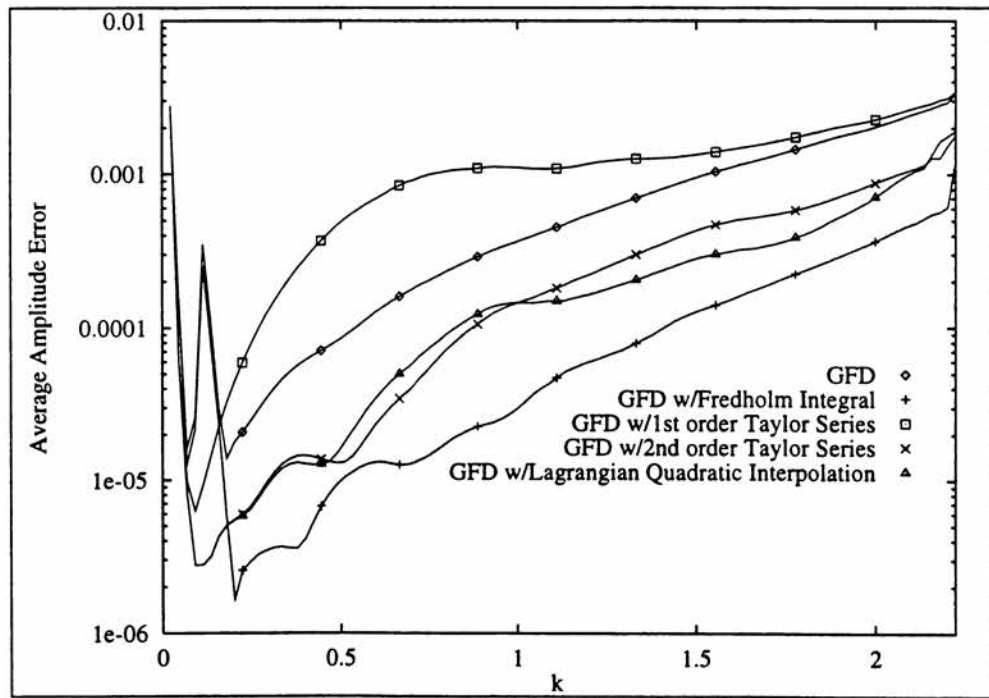


d. average phase error

Figure 9. (continued)

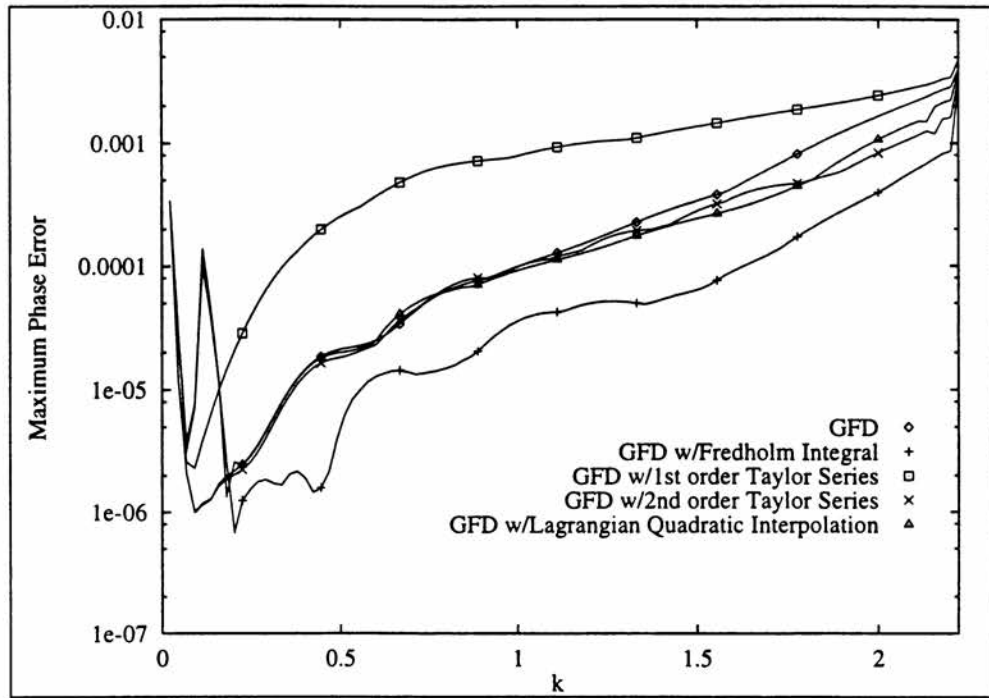


a. maximum amplitude error

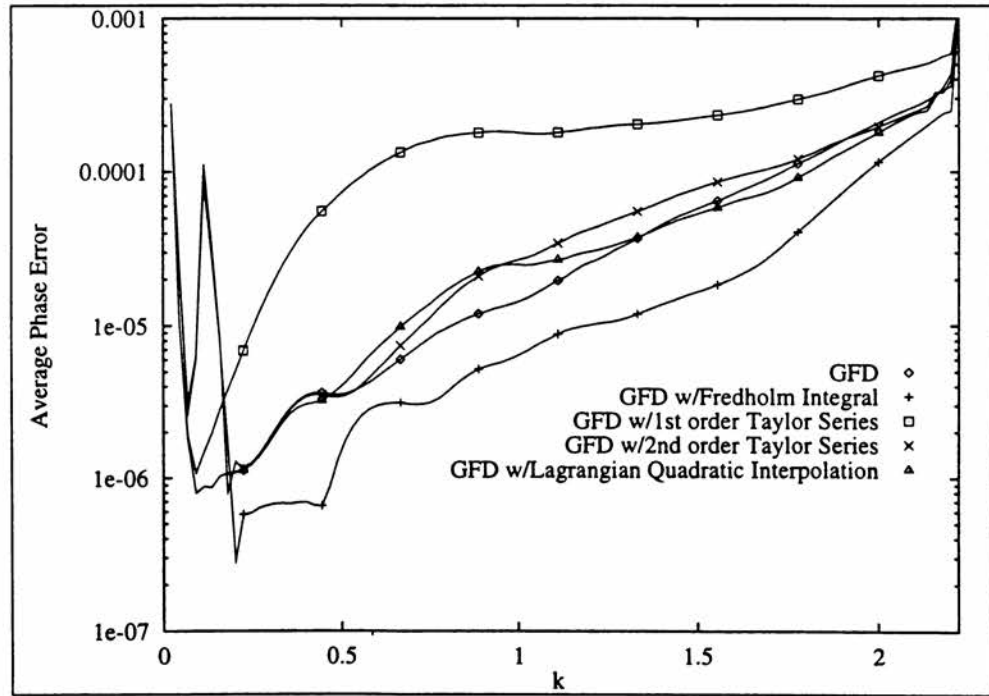


b. average amplitude error

Figure 10. 2-D Method comparison, $H = 0.1$

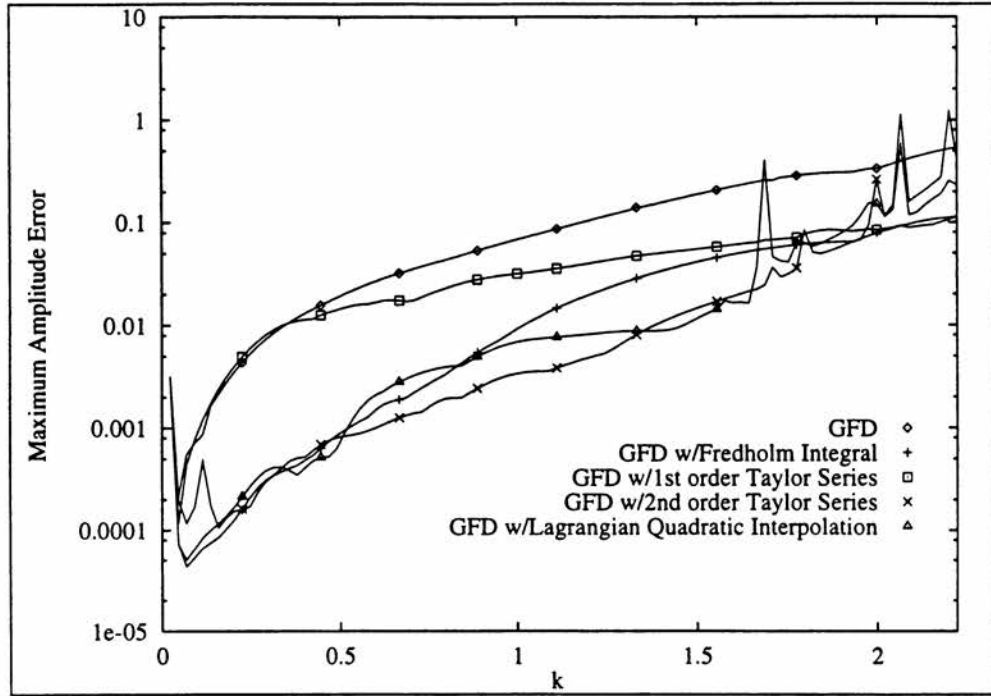


c. maximum phase error

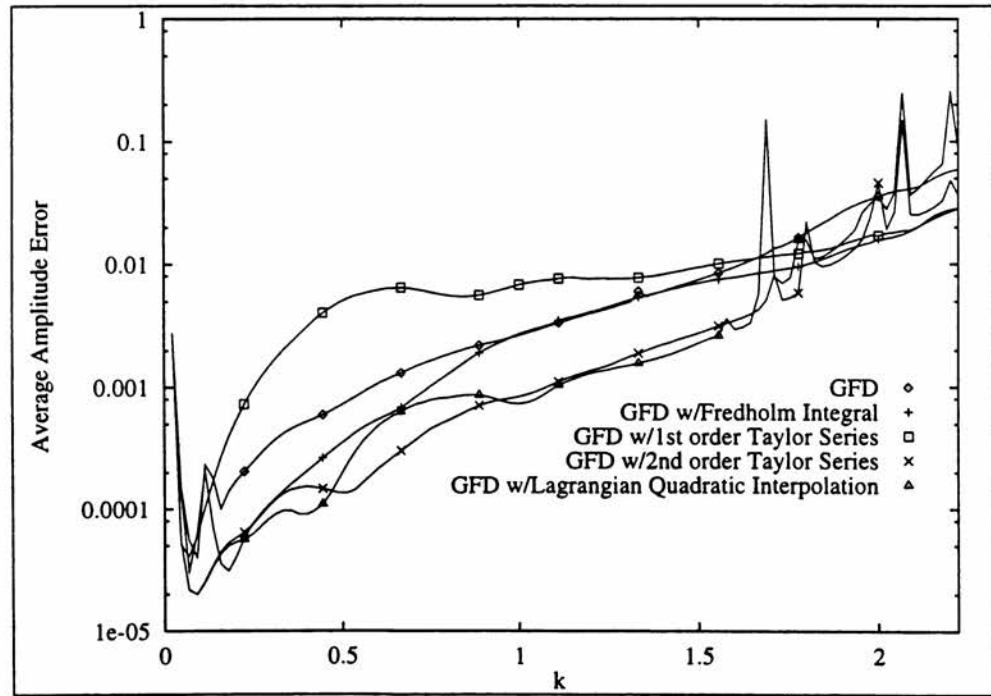


d. average phase error

Figure 10. (continued)

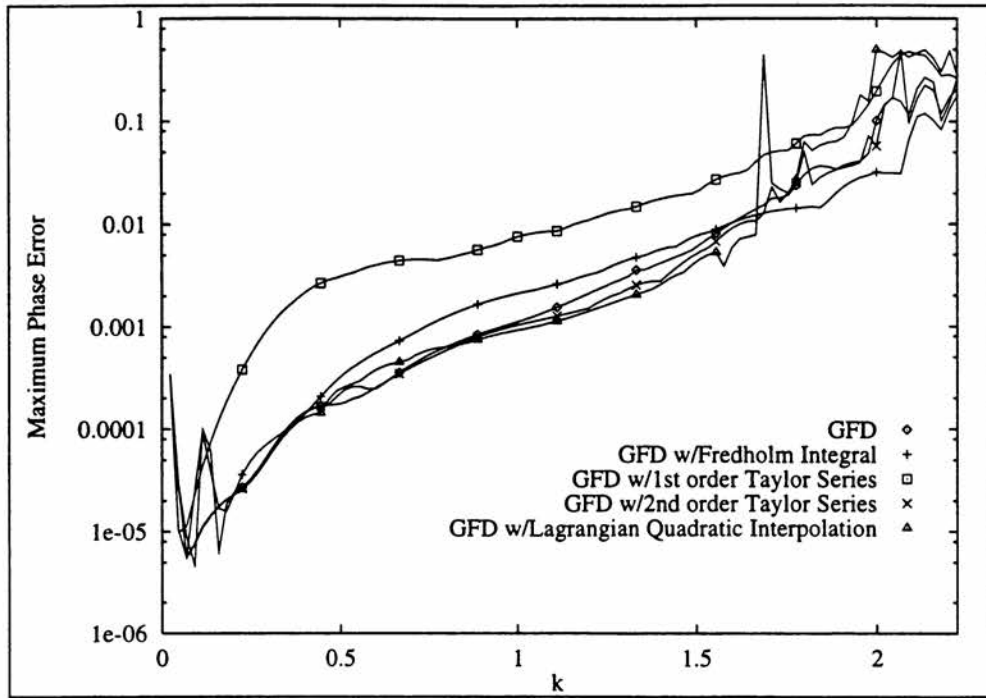


a. maximum amplitude error

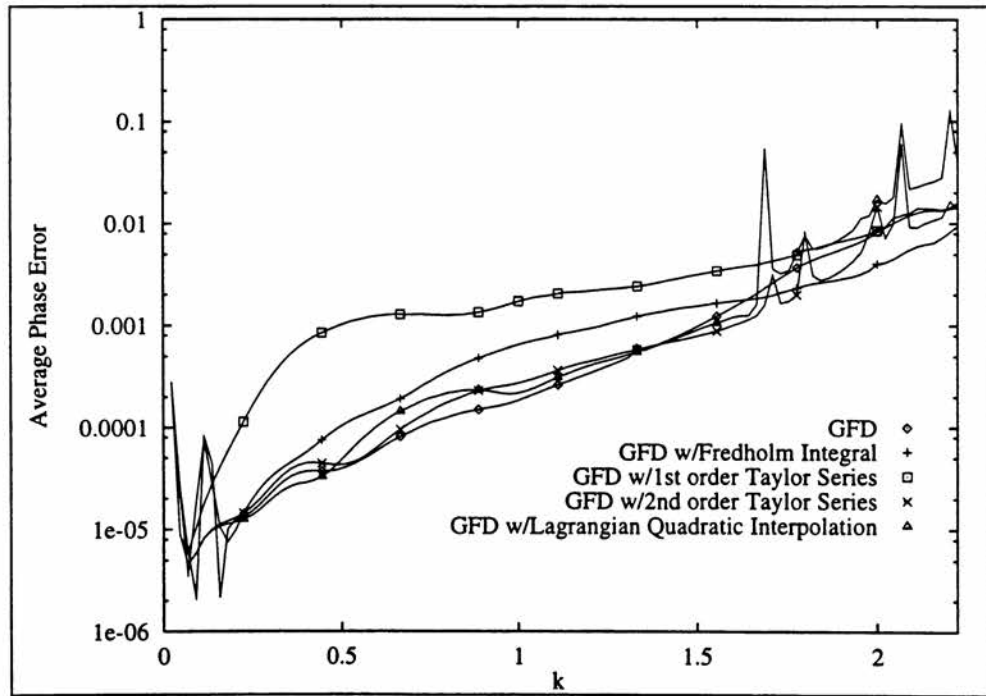


b. average amplitude error

Figure 11. 2-D Method comparison, $H = 1.0$



c. maximum phase error



d. average phase error

Figure 11. (continued)

CHAPTER 4

CONCLUSIONS

Green's Function Discretization has made computationally conceivable fully 3-D frequency domain numerical acoustic computations. First order extensions of GFD to inhomogeneous media have demonstrated a great potential for solving a larger range of real world problems. This dissertation goes one step further, by deriving and demonstrating two second order extensions to increase GFD's accuracy when an inhomogeneous medium is present. Mesh sparseness is the key to making multi-dimensional acoustics problems tractable, and these methods help GFD maintain both its accuracy and its sparseness characteristics. The necessity of the methods presented is determined by both the frequency and steady flow field of interest.

In the course of this investigation, the methods developed for extending GFD to approximate the effects of a second order steady flow field improve both the computed maximum and average amplitude errors in 1-D and 2-D. It was noted that when imparting information concerning inhomogeneous media to a local stencil, only inhomogeneities within stencil bounds needed to be taken into account. Information from outside the local stencil does not need to be included in the GFD process, which greatly simplifies the computational effort required to compute the discretization.

Several observations need to be made concerning the methods examined. It was found for the perturbation expansion method, a first order Taylor series perturbation expansion is not sufficient to account for general variations in the media, whereas a second order Taylor series perturbation expansion yielded excellent results in both one and two dimensions. Also, in terms of computational cost, since the 2nd order Taylor series perturbation expansion is equivalent in accuracy to the quadratic Lagrangian interpolation perturbation expansion, the extra computational work required to compute the Lagrangian correction terms cannot be justified. The Fredholm integral formulation, while more accurate than the particular solution formulation for abrupt changes in the media, requires the evaluation of an integral for each stencil node and single layer potential source strength combination, making the second order Taylor series perturbation expansion method more attractive in terms of the computational effort required.

CHAPTER 5

FURTHER WORK

Further work needs to be conducted to evaluate and extend both the Green's Function Discretization and the correction methods presented in this dissertation. GFD was initially applied to Helmholtz's equation in an attempt to shorten computation times, and it should be applied to other PDEs to see if they can be evaluated with greater accuracy or speed. Also, new means of computing GFD's single layer potential (σ) need to be determined and evaluated. The least-norm least-squares solution found by singular value decomposition yields a unique solution, but it is not the only means to determine σ . To extend GFD even further, it should to be applied in the time domain to solve general wave problems.

The inhomogeneous media correction methods need to be evaluated for 3-D problems, as this is the area in which GFD will make its maximum impact. Finally, the Fredholm integral method needs to be further extended via a transformation that will account for the first order flow variation in the singular Green's function found in the Fredholm integral, so that first order variations in the media can be accounted for exactly.

LIST OF REFERENCES

LIST OF REFERENCES

- [1] Raviprakash, G.K., "A Computational Method for the Analysis of Acoustic Radiation from Turbofan Inlets," Ph.D. Dissertation, The University of Tennessee, Knoxville, May 1992.
- [2] French, J.C., "Evaluation of a Hypothetical Source Method for Discretization of the Helmholtz Equation," M.S. Thesis, The University of Tennessee, Knoxville, December 1993.
- [3] Pierce, A.D., "The Helmholtz-Kirchoff Integral Relation as a Framework for Developing Algorithms for Sound Propagation through Inhomogeneous Moving Media," *Computational Acoustics: Ocean-acoustic Models and Supercomputing, Proceedings of the 2nd IMACS Symposium on Computational Acoustics*, p. 64, 1990.
- [4] Caruthers, J.E., French, J.C., Raviprakash, G.K., "Green Function Discretization for Numerical Solution of the Helmholtz Equation," *Journal of Sound and Vibration*, Vol. 187(4), pp. 553-568, November 9, 1995.
- [5] Caruthers, J.E., Raviprakash, G.K., "A Numerical Solution Method for Acoustic Radiation From Axisymmetric Bodies," Proceedings of the ICASE/LaRC Workshop on Benchmark Problems in Computational Aeroacoustics held at Hampton, VA, October 1994 (NASA Conference Publication 3300), pp. 245-254, May 1995.
- [6] Caruthers, J.E., French, J.C., Raviprakash, G.K., "Recent Developments Concerning a New Discretization Method for the Helmholtz Equation," Proceedings of the 1st CEAS/AIAA Aeroacoustics Conference held at Munich, Germany, CEAS/AIAA paper 95-117, May 1995.
- [7] Caruthers, J.E., Engels, R.C., Raviprakash, G.K., "A Wave Expansion Computational Method for Discrete Frequency Acoustics Within Inhomogeneous Flows," 2nd CEAS/AIAA Aeroacoustics Conference held at State College, PA, CEAS/AIAA paper 96-1684, May 1996.
- [8] Morse, P., Feshback, H., "Methods of Theoretical Physics," McGraw-Hill, NY, part 2, section 9.3.

- [9] Jones, D.S., "Acoustic and Electromagnetic Waves," Oxford Science Publications, Clarendon Press, Oxford, 1986.
- [10] Abramowitz, M., Stegun, I.A., "Handbook of Mathematical Functions", Dover Publications, Inc., New York, 10th printing.
- [11] Caruthers, J.E., and Dalton, W.N., Unsteady Aerodynamics Response of a Cascade to Nonuniform Inflow, "Journal of Turbomachinery", January 1993, vol. 115, no. 1, p. 79.

APPENDICES

APPENDIX A

DERIVATION OF THE ACOUSTIC VELOCITY POTENTIAL EQUATION (AVPE) WITH ISENTROPIC AND IRROTATIONAL STEADY FLOW

This appendix derives the acoustic velocity potential equation, a perturbation expansion of the basic equations of fluid mechanics. It is a completely worked out derivation, formulated previously in [11]. A subscript of 0 defines a parameter as a steady state variable, while a subscript of 1 indicates a perturbation size time dependent quantity.

Euler Equations (no viscosity)

Continuity (ρ is the density, \vec{v} is the velocity vector):

$$\frac{D\rho}{dt} + \rho \nabla \cdot \vec{v} = 0 \quad (\text{A-1})$$

Momentum (p is the pressure):

$$\rho \frac{D\vec{v}}{dt} = -\nabla p \quad (\text{A-2})$$

Energy (s is the entropy):

$$\frac{Ds}{dt} = 0 \quad (\text{A-3})$$

Perturb the parameters accordingly:

$$\rho(x,y,t) = \rho_0(x,y) + \rho_1(x,y,t); \quad \rho_1 \ll \rho_0 \quad (\text{A-4})$$

$$\vec{v}(x,y,t) = \vec{v}_0(x,y) + \vec{v}_1(x,y,t); \quad |\vec{v}_1| \ll c_0 \quad (\text{A-5})$$

$$p(x,y,t) = p_0(x,y) + p_1(x,y,t); \quad |p_1| \ll p_0 \quad (\text{A-6})$$

$$s(x,y,t) = s_0(x,y) + s_1(x,y,t); \quad s_1 \ll s_0 \quad (\text{A-7})$$

Substitute the steady and perturbation variables into the EOM, and factor out the steady portions (set time partial of steady terms to zero):

Continuity:

$$\begin{aligned} \frac{D(\rho_0 + \rho_1)}{dt} + (\rho_0 + \rho_1)\nabla\cdot(\vec{v}_0 + \vec{v}_1) &= 0 \\ \frac{\partial(\rho_0 + \rho_1)}{\partial t} + (v_0 + v_1)\cdot\nabla(\rho_0 + \rho_1) + (\rho_0 + \rho_1)\nabla\cdot(\vec{v}_0 + \vec{v}_1) &= 0 \\ \frac{\partial(\rho_0 + \rho_1)}{\partial t} + \vec{v}_0\cdot\nabla\rho_0 + \vec{v}_0\cdot\nabla\rho_1 + \vec{v}_1\cdot\nabla\rho_0 + \rho_0\nabla\cdot\vec{v}_0 + \rho_0\nabla\cdot\vec{v}_1 + \rho_1\nabla\cdot\vec{v}_0 &= 0 \\ &\quad \text{(A-8)} \\ \frac{\partial\rho_0}{\partial t} + \vec{v}_0\cdot\nabla\rho_0 + \rho_0\nabla\cdot\vec{v}_0 &= 0 \\ \nabla\cdot(\rho_0\vec{v}_0) &= 0 \\ \frac{\partial\rho_1}{\partial t} + \vec{v}_0\cdot\nabla\rho_1 + \vec{v}_1\cdot\nabla\rho_0 + \rho_0\nabla\cdot\vec{v}_1 + \rho_1\nabla\cdot\vec{v}_0 &= 0 \\ \frac{D_0\rho_1}{dt} + \rho_1\nabla\cdot\vec{v}_0 + \nabla\cdot(\rho_0\vec{v}_1) &= 0 \end{aligned}$$

Momentum:

$$\begin{aligned}
(\rho_0 + \rho_1) \frac{D(\vec{v}_0 + \vec{v}_1)}{dt} &= -\nabla(p_0 + p_1) \\
(\rho_0 + \rho_1) \left[\frac{\partial \vec{v}_1}{\partial t} + (\vec{v}_0 + \vec{v}_1) \cdot \nabla (\vec{v}_0 + \vec{v}_1) \right] &= -\nabla(p_0 + p_1) \\
(\rho_0 + \rho_1) \left[\frac{\partial \vec{v}_1}{\partial t} + \vec{v}_0 \cdot \nabla \vec{v}_0 + \vec{v}_0 \cdot \nabla \vec{v}_1 + \vec{v}_1 \cdot \nabla \vec{v}_0 \right] &= -\nabla(p_0 + p_1) \quad (\text{A-9}) \\
\rho_0 \frac{\partial \vec{v}_1}{\partial t} + \rho_0 \vec{v}_0 \cdot \nabla \vec{v}_0 + \rho_1 \vec{v}_0 \cdot \nabla \vec{v}_0 + \rho_0 (\vec{v}_0 \cdot \nabla \vec{v}_1 + \vec{v}_1 \cdot \nabla \vec{v}_0) &= -\nabla(p_0 + p_1) \\
\rho_0 \vec{v}_0 \cdot \nabla \vec{v}_0 &= -\nabla p_0 \\
\rho_0 \left[\frac{D_0 \vec{v}_1}{dt} + \vec{v}_1 \cdot \nabla \vec{v}_0 \right] + \rho_1 \vec{v}_0 \cdot \nabla \vec{v}_0 &= -\nabla p_1
\end{aligned}$$

Energy:

$$\begin{aligned}
\frac{D(s_0 + s_1)}{dt} &= 0 \\
\frac{\partial s_1}{\partial t} + (\vec{v}_0 + \vec{v}_1) \cdot \nabla (s_0 + s_1) &= 0 \\
\frac{\partial s_1}{\partial t} + \vec{v}_0 \cdot \nabla s_0 + \vec{v}_0 \cdot \nabla s_1 + \vec{v}_1 \cdot \nabla s_0 &= 0 \quad (\text{A-10}) \\
\vec{v}_0 \cdot \nabla s_0 &= 0 \\
\frac{\partial s_1}{\partial t} + \vec{v}_0 \cdot \nabla s_1 + \vec{v}_1 \cdot \nabla s_0 &= 0 \\
\frac{D_0 s_1}{dt} + \vec{v}_1 \cdot \nabla s_0 &= 0
\end{aligned}$$

Since $\vec{v}_0 \cdot \nabla s_0 = 0$, either the velocity vector is always perpendicular to the gradient of the

entropy, the velocity vector is zero, or the entropy is constant. We cannot guarantee the relation between the velocity vector and the entropy, nor is the velocity vector always zero, so the steady entropy must be constant (homentropic). The unsteady entropy equation simplifies to:

$$\frac{D_0 s_1}{dt} = 0 \quad (\text{A-11})$$

The unsteady entropy is thus uncoupled from the other unsteady variables and can be solved for separately.

Reiterating, the steady equations are:

$$\nabla \cdot (\rho_0 \vec{v}_0) = 0 \quad (\text{A-12})$$

$$\rho_0 \vec{v}_0 \cdot \nabla \vec{v}_0 = -\nabla p_0 \quad (\text{A-13})$$

$$s_0 = \text{constant} \quad (\text{A-14})$$

The unsteady equations are:

$$\frac{D_0 \rho_1}{dt} + \rho_1 \nabla \cdot \vec{v}_0 + \nabla \cdot (\rho_0 \vec{v}_1) = 0 \quad (\text{A-15})$$

$$\rho_0 \left[\frac{D_0 \vec{v}_1}{dt} + \vec{v}_1 \cdot \nabla \vec{v}_0 \right] + \rho_1 \vec{v}_0 \cdot \nabla \vec{v}_0 = -\nabla p_1 \quad (\text{A-16})$$

$$\frac{D_0 s_1}{dt} = 0 \quad (\text{A-17})$$

Eliminate the perturbed density term, using the relation (c_p is the specific heat with

constant pressure):

$$\rho_1 = \frac{P_1}{c_0^2} - \frac{\rho_0}{c_p} s_1 \quad (\text{A.2})$$

$$\begin{aligned} \frac{D_0}{Dt} \left[\frac{P_1}{c_0^2} - \frac{\rho_0}{c_p} s_1 \right] + \left[\frac{P_1}{c_0^2} - \frac{\rho_0}{c_p} s_1 \right] \nabla \cdot \vec{v}_0 + \nabla \cdot (\rho_0 \vec{v}_1) &= 0 \\ \frac{D_0}{Dt} \left[\frac{P_1}{c_0^2} \right] - \frac{s_1}{c_p} \frac{D_0 \rho_0}{Dt} + \left[\frac{P_1}{c_0^2} - \frac{\rho_0 s_1}{c_p} \right] \nabla \cdot \vec{v}_0 + \nabla \cdot (\rho_0 \vec{v}_1) &= 0 \\ \frac{D_0}{Dt} \left[\frac{P_1}{c_0^2} \right] - \frac{s_1}{c_p} \vec{v}_0 \cdot \nabla \rho_0 + \left[\frac{P_1}{c_0^2} - \frac{\rho_0 s_1}{c_p} \right] \nabla \cdot \vec{v}_0 + \nabla \cdot (\rho_0 \vec{v}_1) &= 0 \\ \vec{v}_0 \cdot \nabla \rho_0 &= -\rho_0 \nabla \cdot \vec{v}_0 \\ \frac{D_0}{Dt} \left[\frac{P_1}{c_0^2} \right] + \frac{P_1}{c_0^2} \nabla \cdot \vec{v}_0 + \nabla \cdot (\rho_0 \vec{v}_1) &= 0 \\ \frac{D_0}{Dt} \left[\frac{P_1}{c_0^2} \right] + \frac{P_1}{\rho_0 c_0^2} \rho_0 \nabla \cdot \vec{v}_0 + \nabla \cdot (\rho_0 \vec{v}_1) &= 0 \\ \frac{D_0}{Dt} \left[\frac{P_1}{c_0^2} \right] - \frac{P_1}{\rho_0 c_0^2} \vec{v}_0 \cdot \nabla \rho_0 + \nabla \cdot (\rho_0 \vec{v}_1) &= 0 \\ \frac{1}{\rho_0} \frac{D_0}{Dt} \left[\frac{P_1}{c_0^2} \right] - \frac{P_1}{\rho_0^2 c_0^2} \vec{v}_0 \cdot \nabla \rho_0 + \frac{1}{\rho_0} \nabla \cdot (\rho_0 \vec{v}_1) &= 0 \\ \frac{D_0}{Dt} \left[\frac{P_1}{\rho_0 c_0^2} \right] &= \frac{1}{\rho_0} \frac{D_0}{Dt} \left[\frac{P_1}{c_0^2} \right] + \frac{P_1}{c_0^2} \frac{D_0}{Dt} \left[\frac{1}{\rho_0} \right] = \frac{1}{\rho_0} \frac{D_0}{Dt} \left[\frac{P_1}{c_0^2} \right] - \frac{P_1}{\rho_0^2 c_0^2} \frac{D_0 \rho_0}{Dt} \\ &= \frac{1}{\rho_0} \frac{D_0}{Dt} \left[\frac{P_1}{c_0^2} \right] - \frac{P_1}{\rho_0^2 c_0^2} \vec{v}_0 \cdot \nabla \rho_0 \\ \frac{D_0}{Dt} \left[\frac{P_1}{\rho_0 c_0^2} \right] + \frac{1}{\rho_0} \nabla \cdot (\rho_0 \vec{v}_1) &= 0 \end{aligned} \quad (\text{A-19})$$

$$\rho_0 \left[\frac{D_0 \vec{v}_1}{Dt} + \vec{v}_1 \cdot \nabla \vec{v}_0 \right] + \left[\frac{p_1}{c_0^2} - \frac{\rho_0 s_1}{c_p} \right] \vec{v}_0 \cdot \nabla \vec{v}_0 = -\nabla p_1$$

$$\rho_0 \left[\frac{D_0 \vec{v}_1}{Dt} + \vec{v}_1 \cdot \nabla \vec{v}_0 - \frac{s_1}{c_p} \vec{v}_0 \cdot \nabla \vec{v}_0 \right] = -\nabla p_1 - \frac{p_1}{c_0^2} \vec{v}_0 \cdot \nabla \vec{v}_0$$

$$\frac{D_0 \vec{v}_1}{Dt} + \left[\vec{v}_1 - \frac{s_1}{c_p} \vec{v}_0 \right] \cdot \nabla \vec{v}_0 = -\frac{1}{\rho_0} \left[\nabla p_1 + \frac{p_1}{c_0^2} \vec{v}_0 \cdot \nabla \vec{v}_0 \right]$$

$$\frac{D_0 \vec{v}_1}{Dt} + \left[\vec{v}_1 - \frac{s_1}{c_p} \vec{v}_0 \right] \cdot \nabla \vec{v}_0 = -\frac{1}{\rho_0} \left[\nabla p_1 - \frac{p_1}{\rho_0 c_0^2} \nabla p_0 \right]$$

(A-20)

$$\nabla \left(\frac{p_1}{\rho_0} \right) = \frac{1}{\rho_0} \nabla p_1 + p_1 \nabla \left(\frac{1}{\rho_0} \right) = \frac{1}{\rho_0} \nabla p_1 - \frac{p_1}{\rho_0^2} \nabla \rho_0 = \frac{1}{\rho_0} \nabla p_1 - \frac{p_1}{\rho_0^2} \nabla \rho_0 \frac{d\rho_0}{dp_0}$$

$$= \frac{1}{\rho_0} \nabla p_1 - \frac{p_1}{\rho_0^2 c_0^2} \nabla p_0$$

$$\frac{D_0 \vec{v}_1}{Dt} + \left[\vec{v}_1 - \frac{s_1}{c_p} \vec{v}_0 \right] \cdot \nabla \vec{v}_0 = -\nabla \left(\frac{p_1}{\rho_0} \right)$$

Reiterating,

$$\frac{D_0}{Dt} \left[\frac{p_1}{\rho_0 c_0^2} \right] + \frac{1}{\rho_0} \nabla \cdot (\rho_0 \vec{v}_1) = 0$$

(A-21)

$$\frac{D_0 \vec{v}_1}{Dt} + \left[\vec{v}_1 - \frac{s_1}{c_p} \vec{v}_0 \right] \cdot \nabla \vec{v}_0 = -\nabla \left(\frac{p_1}{\rho_0} \right)$$

(A-22)

Let

$$\vec{v}_1 = \nabla\phi + \vec{\omega} + \frac{s_1\vec{v}_0}{2c_p} \quad (\text{A-23})$$

ϕ is the acoustic velocity potential, while $\vec{\omega}$ is the perturbed vorticity vector.

$$\begin{aligned} \frac{D_0}{Dt} \left[\nabla\phi + \vec{\omega} + \frac{s_1\vec{v}_0}{2c_p} \right] + \left[\nabla\phi + \vec{\omega} + \frac{s_1\vec{v}_0}{2c_p} - \frac{s_1\vec{v}_0}{c_p} \right] \cdot \nabla\vec{v}_0 &= -\nabla \left(\frac{p_1}{\rho_0} \right) \\ \frac{D_0}{Dt} [\nabla\phi + \vec{\omega}] + \frac{s_1\vec{v}_0}{2c_p} \cdot \nabla\vec{v}_0 + \left[\nabla\phi + \vec{\omega} - \frac{s_1\vec{v}_0}{2c_p} \right] \cdot \nabla\vec{v}_0 &= -\nabla \left(\frac{p_1}{\rho_0} \right) \quad (\text{A-24}) \\ \frac{D_0}{Dt} [\nabla\phi + \vec{\omega}] + [\nabla\phi + \vec{\omega}] \cdot \nabla\vec{v}_0 &= -\nabla \left(\frac{p_1}{\rho_0} \right) \end{aligned}$$

Choose

$$\frac{D_0\vec{\omega}}{Dt} + \vec{\omega} \cdot \nabla\vec{v}_0 = 0 \quad (\text{A-25})$$

Then

If the steady flow is irrotational, $\nabla\vec{v}_0$ is symmetric:

$$\begin{aligned}
\frac{D_0}{Dt}[\nabla\phi] + \nabla\phi \cdot \nabla\bar{v}_0 &= -\nabla\left(\frac{p_1}{\rho_0}\right) \\
\frac{\partial}{\partial t}[\nabla\phi] + \bar{v}_0 \cdot \nabla\nabla\phi + \nabla\phi \cdot \nabla\bar{v}_0 &= -\nabla\left(\frac{p_1}{\rho_0}\right) \\
\frac{\partial}{\partial t}[\nabla\phi] + \nabla\bar{v}_0 \cdot \nabla\phi + \bar{v}_0 \cdot \nabla\nabla\phi + \nabla\phi \cdot \nabla\bar{v}_0 - \nabla\bar{v}_0 \cdot \nabla\phi &= -\nabla\left(\frac{p_1}{\rho_0}\right) \\
\nabla\left[\frac{\partial\phi}{\partial t} + \bar{v}_0 \cdot \nabla\phi\right] + \nabla\phi \cdot \nabla\bar{v}_0 - \nabla\bar{v}_0 \cdot \nabla\phi &= -\nabla\left(\frac{p_1}{\rho_0}\right) \\
\nabla\left[\frac{D_0\phi}{Dt}\right] + \nabla\phi \cdot \nabla\bar{v}_0 - \nabla\bar{v}_0 \cdot \nabla\phi &= -\nabla\left(\frac{p_1}{\rho_0}\right) \\
\nabla\left[\frac{D_0\phi}{Dt}\right] &= -\nabla\left(\frac{p_1}{\rho_0}\right) \\
\frac{D_0\phi}{Dt} &= -\frac{p_1}{\rho_0} + f(t)
\end{aligned} \tag{A-27}$$

The arbitrary function of time is absorbed into phi:

$$\frac{D_0\phi}{Dt} = -\frac{p_1}{\rho_0} \tag{A-28}$$

Furthermore, substituting back into equation 19 (note that this is a different vorticity without entropy term):

If we ignore vorticity altogether:

$$-\frac{D_0}{Dt} \left[\frac{1}{c_0^2} \frac{D_0 \phi}{Dt} \right] + \frac{1}{\rho_0} \nabla \cdot (\rho_0 (\nabla \phi + \bar{\omega})) = 0 \quad (\text{A-29})$$

$$\frac{D_0}{Dt} \left[\frac{1}{c_0^2} \frac{D_0 \phi}{Dt} \right] - \frac{1}{\rho_0} \nabla \cdot (\rho_0 \nabla \phi) = \frac{1}{\rho_0} \nabla \cdot (\rho_0 \bar{\omega})$$

$$\frac{D_0}{Dt} \left[\frac{1}{c_0^2} \frac{D_0 \phi}{Dt} \right] - \frac{1}{\rho_0} \nabla \cdot (\rho_0 \nabla \phi) = 0 \quad (\text{A-30})$$

If the sound is assumed to vary harmonically with time, then, with

$$L = i\alpha + \bar{v}_0 \cdot \nabla \quad (\text{A-31})$$

$$L \{ L(\phi) / c_0^2 \} - \frac{1}{\rho_0} \nabla \cdot (\rho_0 \nabla \phi) = 0$$

$$(i\alpha + \bar{v}_0 \cdot \nabla) \left\{ \frac{i\alpha}{c_0^2} \phi + \frac{1}{c_0^2} \bar{v}_0 \cdot \nabla \phi \right\} = \frac{1}{\rho_0} \nabla \cdot (\rho_0 \nabla \phi) \quad (\text{A-32})$$

$$-\frac{\alpha^2}{c_0^2} \phi + \frac{i\alpha}{c_0^2} \bar{v}_0 \cdot \nabla \phi + \bar{v}_0 \cdot \nabla \left(\frac{i\alpha}{c_0^2} \phi \right) + \bar{v}_0 \cdot \nabla \left(\frac{1}{c_0^2} \bar{v}_0 \cdot \nabla \phi \right) = \frac{1}{\rho_0} \nabla \cdot (\rho_0 \nabla \phi)$$

Let

$$k = \frac{\alpha l}{c_0}, \quad \vec{M}_0 = \frac{\vec{v}_0}{c_0}, \quad \nabla = \frac{1}{l} \nabla' \quad (\text{A-33})$$

$$-\frac{k^2}{l^2} \phi + \frac{ik}{l^2} \vec{M}_0 \cdot \nabla \phi + \frac{1}{l} \vec{v}_0 \cdot \nabla \left(\frac{ik}{lc_0} \phi \right) + \frac{1}{l} \vec{v}_0 \cdot \nabla \left(\frac{1}{lc_0} \vec{M}_0 \cdot \nabla \phi \right) = \frac{1}{l \rho_0} \nabla \cdot \left(\frac{\rho_0}{l} \nabla \phi \right)$$

$$-k^2 \phi + ik \vec{M}_0 \cdot \nabla \phi + i \vec{M}_0 \phi \cdot \nabla k + ik \vec{M}_0 \cdot \nabla \phi - \frac{ik}{c_0} \phi \vec{M}_0 \cdot \nabla c_0 \quad (\text{A-34})$$

$$- \frac{1}{c_0} \vec{M}_0 \cdot \nabla c_0 \vec{M}_0 \cdot \nabla \phi + \vec{M}_0 \cdot \nabla \vec{M}_0 \cdot \nabla \phi + \vec{M}_0 \cdot \nabla \nabla \phi \cdot \vec{M}_0 = \frac{1}{\rho_0} \nabla \rho_0 \cdot \nabla \phi + \nabla^2 \phi$$

$$\begin{aligned} & \left[-k^2 + i \vec{M}_0 \cdot \left(\nabla k - \frac{k}{c_0} \nabla c_0 \right) \right] \phi + \left[2ik \vec{M}_0 - \frac{1}{c_0} \vec{M}_0 \cdot \nabla c_0 \vec{M}_0 + \vec{M}_0 \cdot \nabla \vec{M}_0 - \frac{1}{\rho_0} \nabla \rho_0 \right] \cdot \nabla \phi \\ & = \nabla^2 \phi - \vec{M}_0 \cdot \nabla \nabla \phi \cdot \vec{M}_0 \end{aligned}$$

Note:

$$\vec{v}_0 \cdot \nabla \vec{v}_0 = -\frac{1}{\rho_0} \nabla p_0 = -\frac{c^2}{\rho_0} \nabla \rho_0$$

$$\frac{1}{c_0} \vec{M}_0 \cdot \nabla \vec{v}_0 = -\frac{1}{\rho_0} \nabla \rho_0 \quad (\text{A-35})$$

$$\frac{1}{c_0} \vec{M}_0 \cdot \nabla (c_0 \vec{M}_0) = \frac{1}{c_0} \vec{M}_0 \cdot \nabla c_0 \vec{M}_0 + \vec{M}_0 \cdot \nabla \vec{M}_0 = -\frac{1}{\rho_0} \nabla \rho_0$$

Therefore:

$$\left[-k^2 + i\vec{M}_0 \cdot \left(\nabla k - \frac{k}{c_0} \nabla c_0 \right) \right] \phi + 2[ik\vec{M}_0 + \vec{M}_0 \cdot \nabla \vec{M}_0] \cdot \nabla \phi = \nabla^2 \phi - \vec{M}_0 \cdot \nabla \nabla \phi \cdot \vec{M}_0 \quad (\text{A-36})$$

$$\nabla^2 \phi + k^2 \phi = i\vec{M}_0 \cdot \left[\nabla k - \frac{k}{c_0} \nabla c_0 \right] \phi + 2[ik\vec{M}_0 + \vec{M}_0 \cdot \nabla \vec{M}_0] \cdot \nabla \phi + \vec{M}_0 \cdot \nabla \nabla \phi \cdot \vec{M}_0$$

Note:

$$\frac{k}{c_0} \nabla c_0 = \frac{\alpha l}{c_0^2} \nabla c_0 = -\alpha l \nabla \left(\frac{1}{c_0} \right) = -\nabla \left(\frac{\alpha l}{c_0} \right) = -\nabla k \quad (\text{A-37})$$

This simplifies the equation to:

$$\nabla^2 \phi + k^2 \phi = 2i\phi \vec{M}_0 \cdot \nabla k + 2[ik\vec{M}_0 + \vec{M}_0 \cdot \nabla \vec{M}_0] \cdot \nabla \phi + \vec{M}_0 \cdot \nabla \nabla \phi \cdot \vec{M}_0 \quad (\text{A-38})$$

APPENDIX B

DERIVATION OF THE NTH ORDER ACOUSTIC VELOCITY POTENTIAL PERTURBATION EQUATION

This Appendix follows the perturbation analysis of [7], and is included for the benefit of the reader.

Set the Helmholtz equation in the form

$$A_{ij}\phi_{,ij} + B_i\phi_{,i} + C\phi = 0 \quad (\text{B-1})$$

A_{ij} , B_i , and C are spatially varying parameters. To separate the non-constant coefficient PDE into a constant coefficient PDE with forcing functions, perturb the acoustic potential and the coefficient values. A^0 , B^0 and C^0 are defined at the stencil's computed node, and A^1 , B^1 and C^1 will be the variation from the constant terms:

Substitute these quantities into the non-constant coefficient Helmholtz Equation (1):

$$\begin{aligned}
\phi &= \phi^0 + \varepsilon\phi^1 + \varepsilon^2\phi^2 + \dots \\
A_{ij}(x,y) &= A_{ij}^0(x_0,y_0) + \varepsilon A_{ij}^1(x,y) \\
B_i(x,y) &= B_i^0(x_0,y_0) + \varepsilon B_i^1(x,y) \\
C(x,y) &= C^0(x_0,y_0) + \varepsilon C^1(x,y)
\end{aligned} \tag{B-2}$$

$$\begin{aligned}
&(A_{ij}^0 + \varepsilon A_{ij}^1)(\phi^0 + \varepsilon\phi^1)_{,ij} + (B_i^0 + \varepsilon B_i^1)(\phi^0 + \varepsilon\phi^1)_{,i} \\
&+ (C^0 + \varepsilon C^1)(\phi^0 + \varepsilon\phi^1) = f
\end{aligned} \tag{B-3}$$

Collect like terms of ε :

$$A_{ij}^0\phi_{,ij}^0 + B_i^0\phi_{,i}^0 + C^0\phi^0 = 0 \tag{B-4}$$

$$A_{ij}^0\phi_{,ij}^1 + B_i^0\phi_{,i}^1 + C^0\phi^1 = -[A_{ij}^1\phi_{,ij}^0 + B_i^1\phi_{,i}^0 + C^1\phi^0] \tag{B-5}$$

or in general,

$$A_{ij}^0\phi_{,ij}^{n+1} + B_i^0\phi_{,i}^{n+1} + C^0\phi^{n+1} = -[A_{ij}^1\phi_{,ij}^n + B_i^1\phi_{,i}^n + C^1\phi^n], \quad n \geq 0 \tag{B-6}$$

APPENDIX C

DERIVATION OF THE PARTICULAR SOLUTION TO 2-D QUADRATIC LAGRANGIAN INTERPOLATION FUNCTIONS

This Appendix demonstrates how when a 2-D quadratic Lagrangian function is used to model the second order perturbations in the flow properties to the acoustics, a particular solution can be formed. The function P is thus chosen to be:

$$P(x,y) = p_0 + p_1x + p_2y + p_3x^2 + p_4xy + p_5y^2 + p_6x^2y + p_7xy^2 + p_8x^2y^2 \quad (\text{C-1})$$

The R polynomial to be used must be chosen; it will be expressed using r_i coefficients:

$$R(x,y) = r_0 + r_1x + r_2y + \dots = [1,x,y,\dots] \cdot \vec{r} \quad (\text{C-2})$$

Three rules will be employed to assist in finding a combination of terms that will yield

a potentially invertible system of equations to solve for the particular solution's coefficients (\vec{r}):

Rule #1: The R terms' derivatives must contain the set of P terms. The homogeneous PDE's exponential solution is of the same as form as the forcing function's exponential term, so the particular solution must contain polynomial terms that are one order higher than the highest forcing function polynomial.

Rule #2: The number of r coefficients equals the number of R's unique polynomial derivative terms, to avoid singular matrices when solving for the undetermined coefficients.

Rule #3: Every polynomial term (including derivatives) must be repeated at least once if it does not have a corresponding P polynomial term.

Rule #4: The resulting system of equations to determine R's coefficients may or may not yield a solution for all plane wave directions. To ensure that the matrix is invertible in all circumstances, choose a plane wave's direction vector to parallel the x axis, set $a_y = 0$, and compute the determinant.

The highest order term of P is the x^2y^2 term, a fourth order term. Rule #1 dictates that the highest order terms of R must be fifth order terms. Also from Rule #1, the derivatives of R must include the set:

$$[x, y, x^2, xy, y^2, x^2y, xy^2, x^2y^2] \quad (\text{C-3})$$

To determine which polynomial terms to include, examine the following list of potential terms and their derivatives to include. Combinations of the derivative terms are the only ones that can be considered to match with the forcing function terms, because the non-derivative terms sum to zero:

#	<i>term</i>	<i>derivatives</i>
1)	1	0
2)	x	1
3)	y	1
4)	x ²	1 x
5)	xy	1 x y
6)	y ²	1 y
7)	x ³	x x ²
8)	x ² y	x y x ² xy
9)	xy ²	x y xy y ²
10)	y ³	y y ²
11)	x ⁴	x ² x ³
12)	x ³ y	x ² xy x ³ x ² y
13)	x ² y ²	x ² xy y ² x ² y xy ²
14)	xy ³	xy y ² xy ² y ³
15)	y ⁴	y ² y ³
16)	x ⁵	x ³ x ⁴
17)	x ⁴ y	x ³ x ² y x ⁴ x ³ y
18)	x ³ y ²	x ³ x ² y xy ² x ³ y x ² y ²
19)	x ² y ³	x ² y xy ² y ³ x ² y ² xy ³
20)	xy ⁴	xy ² y ³ xy ³ y ⁴
21)	y ⁵	y ³ y ⁴

From rule #3, all six terms from the fifth order set (16-21) must be included in the set of R terms. These yield nine unique derivative terms, each of which is repeated within the set. The derivatives also cover 3 terms of P (rule #1). There is some freedom in the selection of the rest of the R terms.

Now rule #2 must be applied. It is necessary to find a set of R polynomial terms which have the same number of terms as unique derivatives. Possible sets are:

[2-10,16-21]

[4,6,8,9,11-21]

[4,6,7,10-21]

[4,6,7-10,12-14,16-21]

The only set that satisfies rule #4 is [4,6,7,10-21]. This is a set of 15 polynomial terms that have 15 unique derivatives, each of which is repeated at least once for non-P polynomial terms (actually, each term is repeated even if it appears in P).

The chosen form of R and its derivatives:

$$R(x,y): [x^2, y^2, x^3, y^3, x^4, x^3y, x^2y^2, xy^3, y^4, x^5, x^4y, x^3y^2, x^2y^3, xy^4, y^5] \quad (C-5)$$

$$R_x(x,y): [2x, 0, 3x^2, 0, 4x^3, 3x^2y, 2xy^2, y^3, 0, 5x^4, 4x^3y, 3x^2y^2, 2xy^3, y^4, 0] \quad (C-6)$$

$$R_{xx}(x,y): [2, 0, 6x, 0, 12x^2, 6xy, 2y^2, 0, 0, 20x^3, 12x^2y, 6xy^2, 2y^3, 0, 0] \quad (\text{C-7})$$

$$R_{yy}(x,y): [0, 2y, 0, 3y^2, 0, x^3, 2x^2y, 3xy^2, 4y^3, 0, x^4, 2x^3y, 3x^2y^2, 4xy^3, 5y^4] \quad (\text{C-8})$$

$$R_{xy}(x,y): [0, 2, 0, 6y, 0, 0, 2x^2, 6xy, 12y^2, 0, 0, 2x^3, 6x^2y, 12xy^2, 20y^3] \quad (\text{C-9})$$

$$R_{xy}(x,y): [0, 0, 0, 0, 0, 3x^2, 4xy, 3y^2, 0, 0, 4x^3, 6x^2y, 6xy^2, 4y^3, 0] \quad (\text{C-10})$$

A system of equations can be established by associating like R polynomial terms by row in their R vector location with the corresponding P polynomial term on the right hand side:

Once \bar{r} is solved for, the R function is known and can be used to modify the discretization function as described in Section 2.2.

VITA

Jonathan Charles French was born in Buffalo, New York on May 22, 1969. He graduated from Windsor High School in Windsor, Connecticut in May, 1987. The following September he entered Worcester Polytechnic Institute in Worcester, Massachusetts and in May, 1991, received the degree of Bachelor of Science in Mechanical Engineering. In September, 1991, he entered The University of Tennessee Space Institute (UTSI), in Tullahoma, Tennessee and in December, 1993, received a Master of Science degree in Mechanical Engineering. He continued his research at UTSI, and received his Doctor of Philosophy degree in Engineering Science in December, 1996.